Sodium Percarbonate Fuel Cells Based on Porous Paper Supports

A Project Report Submitted

as part of the requirements for the degree of

MASTER OF SCIENCE

By

RAJAT VERMA

(Roll No. CY14MSCST11012)

Under the supervision of

Dr. M. Deepa
Dr. Kirti Chandra Sahu
Dr. Vinod Janardhanan

भारतीय प्रौद्योगिकी संस्थान हैदराबाद
Indian Institute of Technology Hyderabad

to the

DEPARTMENT OF CHEMISTRY

INDIAN INSTITUTE OF TECHNOLOGY HYDERABAD

INDIA

APRIL, 2016

Declaration

I hereby declare that the matter embodied in this report is the result of investigation carried out by me in the Department of Chemistry, Indian Institute of Technology Hyderabad under the supervision of *Dr. M. Deepa, Dr. Kirti Chandra Sahu* and *Dr. Vinod Janardhanan*.

In keeping with general practice of reporting scientific observations, due acknowledgement has been made wherever the work described is based on the findings of other investigators.
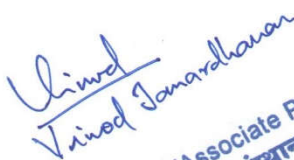
(M DEEPA)

Signature of the Supervisors

Dr. M. Deepa
Head & Associate Professor
Department of Chemistry
Indian Institute of Technology Hyderabad
Kandi-502285, Sangareddy, Telangana, India

(Signature)

RAJAT VERMA

CY14MSCST11012

Department of chemistry

Dr. Kirti Chandra Sahu
Head & Associate Professor
Department of Chemical Engineering
Indian Institute Technology Hyderabad
Kandi, Sangareddy - 502285, Telangana, India

Vinod Janardhanan

सह प्रोफेसर /Associate Professor
भारतीय प्रौद्योगिकी संस्थान हैदराबाद
Indian Institute of Technology Hyderabad
Kandi, Sangareddy - 502 285, Telangana, India

(i)

Approval Sheet

This thesis entitled "**Sodium Percarbonate Fuel Cells Based on Porous Paper Supports**" by **Rajat Verma** is approved for the degree of Master of Science from IIT Hyderabad.

Dr. SURENDRA K. MARTHA
Assistant Professor
Department of Chemistry
Indian Institute of Technology Hyderabad

-Name and affiliation-

Examiner

सह प्रोफेसर /Associate Professor
भारतीय प्रौद्योगिकी संस्थान हैदराबाद
Indian Institute of Technology Hyderabad
Kandi, Sangareddy - 502 285, Telangana, India

-Name and affiliation-

Examiner

Dr. M. Deepa
Head & Associate Professor
Department of Chemistry
Indian Institute of Technology Hyderabad
Kandi-502285, Sangareddy, Telangana, India

-Name and affiliation-

Adviser

Dr. Kirti Chandra Sahu
Head & Associate Professor
Department of Chemical Engineering
Indian Institute Technology Hyderabad
Kandi, Sangareddy - 502285,Telangana, India

-Name and affiliation-

Co-Adviser

Vinod Janardhanan

सह प्रोफेसर /Associate Professor
भारतीय प्रौद्योगिकी संस्थान हैदराबाद
Indian Institute of Technology Hyderabad
Kandi, Sangareddy - 502 285, Telangana, India

-Name and affiliation-

Co-Adviser

-Name and affiliation-

Chairman

(ii)

Acknowledgement

I would like to express my earnest gratitude to my supervisor **Dr. M. Deepa, Dept. of chemistry**, and my co-supervisors **Dr. Kirti Chandra Sahu, Dept. of Chemical Engineering**, and **Dr. Vinod Janardhanan, Dept. of Chemical Engineering**, for providing me an opportunity to work on Fuel cells and their continuous support for research, patience, motivation, and immense knowledge.

I am very grateful to all of them, whose expertise, understanding and generous guidance and support made it to work on the fuel cell that was of great interest to me. The door to all the supervisor' office was all the time remained open when I had any problem or query related to my research work or writing. Their guidance has always redound me at every time of this project and writing of this thesis. I could not have imagined, having these better advisors and mentors for my M.Sc project.

Furthermore I would like to thank **Ms. Sweta Lal, PhD scholar** for introducing me to the topic as well for the support on the way.

I want to thank to all my lab-mates for joyful moments, help and discussion.

I would like to express my thankfulness to all my teachers who put their faith in me and urged me to do better.

Last but not least, I want to express my very eminent indebtedness to my parents and to my friends for providing me with inexhaustible support and endless Impulsion throughout this project study. This proficiency would not have been presumable without them. Thank you.

Author

RAJAT VERMA

Table of content

List of figures

Abstract

A self-pumping T-shaped paper based fuel cell was fabricated using sodium percarbonate as a fuel and potassium permanganate as an oxidant. The cell is portable, economic, lightweight and compact, consumes less fuel, and can be easily regenerated. Whatman filter papers served as porous supports for fluids. Different electrolytes (for fuel and oxidant) and different gel electrolytes were attempted. Among acidic media, mixed media and basic media, the mixed media combination outperforms both acidic and basic media combinations. A T-shaped mixed media paper based fuel cell at 3 M sodium percarbonate (SPC) as fuel concentration produces OCV of 1.22 V. It generates a maximum current density of 3.21 mA/cm^2 and a maximum power density of 1.2 mW/cm^2 at optimum fuel (3 M SPC) concentration without any catalyst. Au NPs were used as catalyst, and the maximum current and maximum power densities increased to 5.357 mA/cm^2 and 2.15 mW/cm^2 respectively. A 66.67 % increment was observed for maximum current density and 79.16 % increment was observed for maximum power density with Au NPs as catalyst, at 3 M optimum fuel concentration. Au/NiO composites as catalysts, further increase the performance of cell. Implementation of Au/NiO as catalysts on the T-shaped mixed media cell, gives maximum current and power densities of 5.625 mA/cm^2 and 2.66 mW/cm^2 respectively, at 3 M optimum concentration of SPC fuel, with increase in the maximum current density by 75 % and maximum power density by 122 % respectively. Electrochemical impedance spectroscopy analysis showed that the anodic polarization resistance decreases with increase in SPC fuel concentration and at constant oxidant concentration.

Chapter 1

Introduction to fuel cells

Introduction to fuel cells

A fuel cell is an electrochemical cell which converts chemical energy directly into electrical energy via redox reactions without being converted into heat and mechanical energy. Fuel cell generates electrical energy by chemical reaction, without the combustion of fuel [6]. It produces electricity, water and heat by the conversion of hydrogen and oxygen into water. The reaction takes place at electrodes, the one which is positive and on which reduction takes place is called as cathode and the other negative electrode where oxidation of the fuel takes place is called as an anode. A separator is placed between these electrodes. Electrons flows from anode to cathode through an external circuit and completes a circuit.
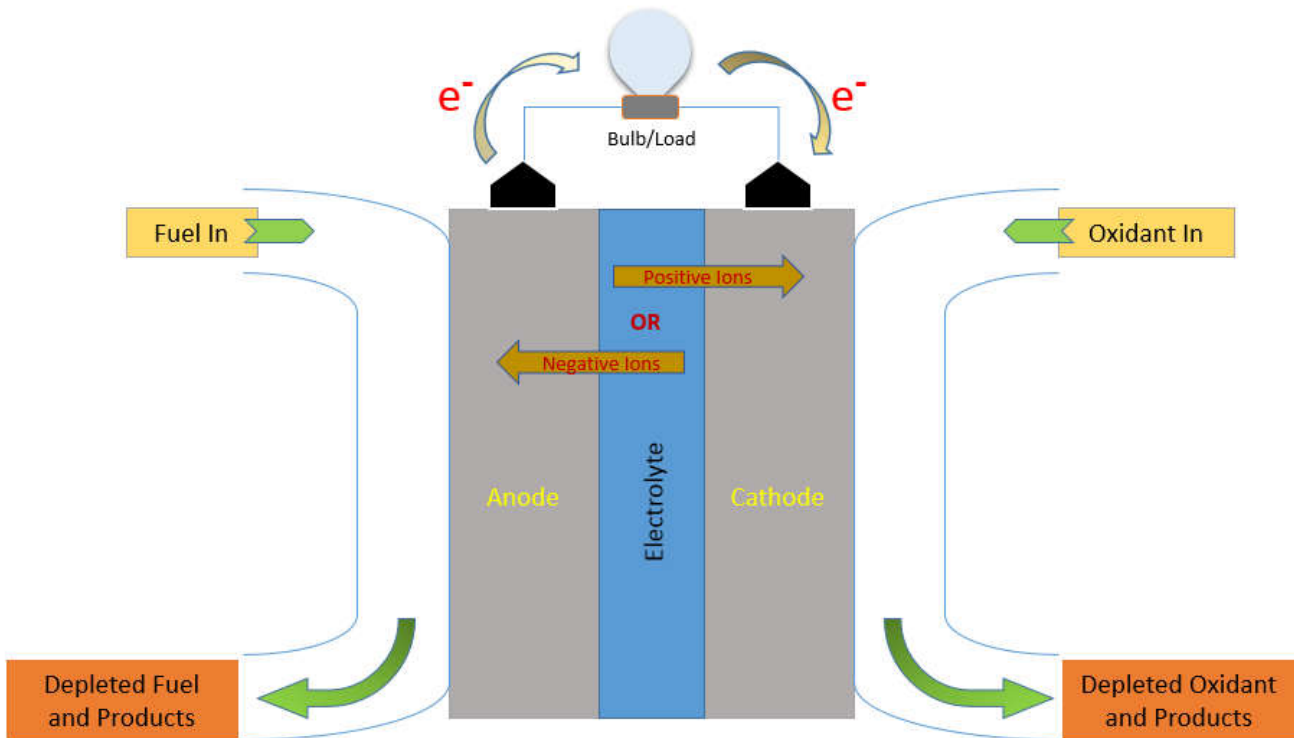
Fig.1 General representation of fuel cell

The basic fuel for a fuel cell is hydrogen but they also require oxygen as an oxidant. It is the combination of the fuel-oxidant that gives a desirable output. Fuel cells generate power with

very less or almost no pollution, and much of the hydrogen and oxygen is used to generate electricity which reacts and combines to give water as harmless byproduct [6].

Operation and generation of electrical power by fuel cell is closely similar to that of the batteries, except they are not rechargable. The main difference between batteries and fuel cells is that battery stores chemicals inside and by chemical reactions produces electricity [2] while fuel cells need continuous fuel supply. Once chemicals runs out from the battery after reactions it expires, but fuel cell stay as long as the fuel is endowed to the system. Though the demand may for an iPOD, cell phone or laptop, buyer demands for a longer life cell with small designed and lower cost energy source. Area of fuel cells is gaining prodigious importance for high power electricity generation, for transportation vehicles due to permissive environment friendly operations. In 2015, some of fuel cell vehicles have been proposed commercially: (1) Toyota Mirai and (2) Hyundai ix35 FCEV. The Honda FCX Clarity, and Mercedes-Benz F-Cell models [3].

Benefits of fuel cells:

1) Environmental: hydrogen fuel cells do not produce air pollutants or green-house gases [6].
2) Energy efficient: Fuel cells are two to three times more dexterous than combustion engines.
3) Versatile: scalable and provide power from milliwatts to megawatts.
4) Fuel flexible: Fuel cells can operate in a neat mode using various fuels including
   methanol, hydrogen, ethanol and formic acid etc. [1].
5) Supplementary: Fuel cell can be easily combined with other energy conversion technologies.

1.1 History of fuel cells

In the mid of 19th century, There were quite some controversies regarding the invention of fuel cell principle. In accordance with Department of Energy of the United States, the German chemist Christian Friedrich Schonbein, consolidated the maiden scientific research on a fuel cell in 1838, and his work was published on January 1839 in The London and Edinburgh Philosophical Magazine and Journal of Science. He examined the first crude fuel and claimed that current was produced from hydrogen and oxygen dissolved in water. In contradiction, the author affirmed in references that it was Sir *William Robert Grove*, who proposed the first concept of hydrogen fuel cell [1] [4].

The first reference of hydrogen fuel cells came out in 1838. The letter was dated in October 1838 however got published on December 1838, in same magazine, The London and Edinburgh Philosophical Magazine and Journal of Science. Sir William Robert Grove researched that by dipping two platinum electrodes such that one end of both stays in a solution of sulfuric acid and another ends of both electrode are sealed separately with hydrogen and oxygen gases, he observed a constant current was flowing between these electrodes. Respective containers were found to contain water along with gases. Grove saw that water level in both containers rose with increase in current. He afterwards observed the higher voltage drop when combining two electrodes in series connection, and this was called by him as gas battery, i.e. the first fuel cell [4].

Year

1800: W. Nichols and A. Carlisle described the electrolysis of water, which was an opposite

process to the one observed in the hydrogen fuel cell [4].

1838: W. Robert Grove designed the first "gas battery", first fuel cell.

1889: Ludwig Mond and Car Langer mentioned the procedure for gaining nickel-Mond

process, and incited the Mond experiment with fuel cells.

1893: Friedrich Wilhelm Ostwald, experimentally determined the connection of different

parts of a fuel cell and the theoretical description about the electrochemical

performances of fuel cell.

1896: William W. Jacques created the first fuel cell for practical application.

1900: Walther Nernst, used zirconium as solid electrolyte.

1921: Emil Baur created the first molten carbonate fuel cell.

1930: E. Baur used solid oxide electrolytes for high temperature.

1939: Thomas Francis Bacon introduces his work by examining alkaline fuel cells and
fabricated cells with using non-novel metal electrodes i.e. nickel electrodes. During 2nd
World War, he designed a fuel cell which was used in submarines of the Royal Navy.

1950: Teflon was used in platinum/acid and carbon/alkaline fuel cells.

1955: Thomas Grubb modified the cell design by using ion-exchange polystyrene sulfonate
membrane. T. Grubb and L. Niedrach develop the PEMFC technology at General
Electric.

1958: G. H. J. Broers and J. A. ketelaar constructed the Molten Carbonate fuel cell.

1959: Francis Bacon proved a 5KW alkaline fuel cell.

1960: Fuel cells were used by NASA for the first time in space mission. PEMFC was invented
by the company GE with the work done by T. Grubb and L. Niedrach.

1961: G.V. Elmore and H.A. Tanner introduced a phosphoric acid fuel cell.

1980: US Navy uses Fuel cells in submarines.

1990: NASA Jet Propulsion Lab and Southern California University developed a direct
methanol fuel cell.

2000: Fuel cell commercialization.

2007: Honda announced first fuel cell car (FCX clarity) [4].

2015: Toyota Mirai and Hyundai ix35 FCEV, proposed commercially in the market for rent
but in finite numbers [2].

1.2 Types of fuel cells and their application

Fuel cells are generally have three essential adjacent components: Anode, cathode and electrolyte. The type of fuel cell depends upon the designed features i.e. usually the type of electrolyte used and the fuel used [28].
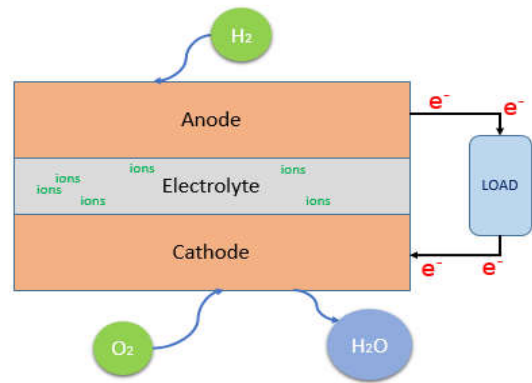
Fig 1.2 Block diagram of fuel cell

1.2.1 Polymer Electrolyte Membrane Fuel Cell (PEMFC)

These are low temperature fuel cells, operate at 60-80 °C temperatures. Hydrogen is used as a typical fuel, originated from a tincture of water and lithium hydroxide, which was provided through bottles. Nafion is used as an electrolyte and graphite are the electrodes with platinum as catalyst for both. Due to Pt, the price of system raised. Charge carrier is H^+ and CO & H_2S are major contaminants in this system [4].

Electrical efficiency: 40-60 % [28]   Power: 50 W to 75 kW [4].

Advantages:

❖ High power density and compact structure, rapid start up due to low temperature operation.

❖ Use of non-corrosive electrolyte. Discard the need of handling acids or any other corrosive and increased security.

Disadvantages:

❖ They are costly due to platinum as catalyst and a solid polymer membrane.

❖ Very sensitive, do not bear CO level more than 50 ppm.

1.2.2 Alkaline Fuel Cell (AFC)

These operate in the temperature range of 65 °C to 220 °C at 1 atm pressure. Unlike PEM, the electrolyte helps to transport hydroxide ions (OH^-) to the anode by cathode. KOH solution and anion exchange membrane are used as electrolytes. Use of nickel and silver both supported on

(6)

carbon as catalyst for anode and cathode respectively. CO_2 contamination responsible for the decay in performance of system [4] [28].

Electrical efficiency: 60-70 % [28]   Power: 300 W to 5 kW [4].

Advantages:

- ❖ They are highly efficient and have catalyst flexibility.
- ❖ Use only small quantities of catalysts, which decreases costs.

Disadvantages:

- ❖ These are extremely sensitive to CO_2 (up to 350 ppm) and less to CO.
- ❖ For mobile electrolyte systems, management becomes complex.

1.2.3 Phosphoric Acid Fuel Cell (PAFC)

In this type of cell, concentrated liquid phosphoric acid (H_2SO_4) in silicon carbide (SiC) is used as the electrolyte. They operate nearly at 150–200 ˚C and at atmospheric pressure. Every cell is be able to produce around 1.1 V. Carbon monoxide level more than 1.5% cannot be tolerated by these cells. In such cells, protons are the charge carriers which travel from the anode to cathode through the electrolyte. Platinum is used as a catalyst and it is supported on carbon / graphite [4] [28].

Electrical efficiency: reaches up to 40 %

Advantages:

- ❖ The cell is full-fledge and reliable.
- ❖ Better tolerant to contaminants: CO_2, Siloxane and H_2S.

Disadvantages:

- ❖ Liquid acidic electrolytes are used which are corrosive and tough to handle.
- ❖ The have an operating temperature to run the cell. Also they are heavy and big.

1.2.4 Molten Carbonate Fuel Cell (MCFC)

These cells contain liquid alkali carbonate (Li_2CO_3, Na_2CO_3 etc.) in lithium aluminate ($LiAlO_2$) as electrolyte. These cells works at high temperature, 600-700 ˚C and high pressures, 1 to 10 atm. The main charge carriers are carbonate ions (CO_3^{-2}) and they move from the cathode to

the anode. They require oxygen and carbon dioxide as fuel and cell gives voltages in between 0.7 V to 1 V.

Anode: Nickel Chromium (NiCr) and Cathode: Lithiated nickel oxide (NiO) are supported on stain less steel. Sulfide and halides are major contaminants for these cells [4] [28].

Electrical efficiency: 55-65 %   Power: 10 KW to 2 MW.

Advantages:

- ❖ High Electrical efficiency, high speed of reaction and good grade heat.
- ❖ Fuel flexibility and inexpensive catalyst is used, so cost of the cell is reduced.

Disadvantages:

- ❖ Corrosion of electrolytes and handling is tough due to the corrosive nature and corrosion of metal occurs.
- ❖ Require preheating before the startup of the cell.

1.2.5 Solid Oxide Fuel Cell (SOFC)

In this type of cell, solid oxide electrolytes of zirconium, lanthanum or yttrium are used. These are also high temperature Fuel cells which operate between 800 -1000 °C. Electrolyte conducts O^{-2} from the cathode to the anode and ceramics are the interconnect materials for electrode support. Sulfides act as contaminants for the cell and are responsible for performance decay.

Anode: Nickel-Solid yttria stabilized zirconia (YSZ) composite.

Cathode: Strontium-doped lanthanum manganite (LSM) [4] [28].

Electrical efficiency: 55-65 %

Advantages:

- ❖ Inexpensive catalyst and fuel flexibility.
- ❖ Electrolytes are solids and handling is easy.

Disadvantages:

- ❖ Sealing and Durability issues. High cost setup.
- ❖ Low power density.

1.2.6 Paper based fuel cell

In the early 21st century, paper based fuel cells emerged and this field is now witnessing many new developments. These fuel cells rely on laminary flow of liquids in paper, which is a porous material and due to its' porosity and capillarity, two parallel flowing streams of anolyte and catholyte, with or without a membrane can be achieved. This cell works under room temperature and 1 atm pressure. The fuel and oxidant are fed on the paper, according to requirement, they either sometimes need micro pumps or no pump is used because reactants flow due to the capillary action of paper. But change in flow rate of fuel & oxidant affects the performance of the cell. Fuel and oxidant are liquids. Since last decade, lateral flow strips are used for diagnostic purposes for biological samples. Therefore keeping this in mind, paper based fuel cells were introduced. These cells are capillary-based systems and can deliver power in the range of mW to micro-W per sq cm to power micro-nano systems which can assess biological samples [5].

Voltage: mV to V   Current: mill-ampere's   Power: mill-watt

Advantages:

❖ Portable, light weight as well as cost-effective cells.
❖ Electrolyte and fuel flexibility.
❖ Cheap metal catalysts or composites, non-metallic nanostructured catalysts can be used.

Disadvantages:

❖ Power and current densities are low.
❖ Contamination of other substance rather than diagnosing sample, produce false result under the same experiment. So these are very sensitive.

1.3 Advantages and future benefits

From the results of last few decades, the fuel cell technology is showing a highly improved development in the area of power generation. Due to high efficiency conversion of chemical energy directly to electrical energy without the combustion of fuel, fuel cells would be promising power source for next generation. Since the thermodynamic laws do not govern fuel

cells, such as Carnot efficiency associated with heat engines, it attains high efficiency in terms where waste heat from cell is used in cogeneration situation [28].

The high power density of the cell allows it to serve as a compact electric power source which is beneficial in automobiles, forklifts, submarines, remote areas of military as well as space constraints etc. Fuel cells do not produce noise during power production, therefore these cells can be used in residential or built-up areas and hospitals where noise pollution is objectionable and troublesome.

The basic fuel is hydrogen which is pollution free, has highest energy content, and gives off only electricity, with heat and water as byproducts. Fuel cells offer an alternative to generating new power production technology which is quiet, versatile, energy efficient, environment friendly and complementary to other power generating devices etc.

Chapter 2

Fundamental terms used for fuel cells

Fundamental terms used for fuel cells

There are some fundamental terms used for fuel cells:

2.1 OCV: Open Circuit Voltage

The open circuit voltage is the maximum available voltage when no current is flows through the circuit [7]. There is no load connected and circuit is not closed i.e. electrical path is not complete. Represented by the symbol V_{oc}.
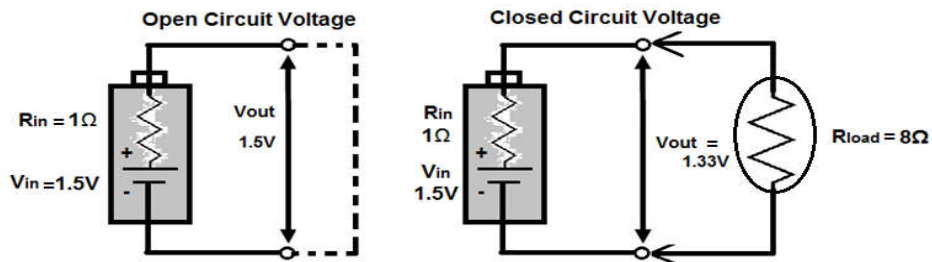
2.1 Diagram for open and closed electrical circuit

2.2 Current density and power density

Current Density: It is the ratio of electric current passing through the conductor to the area of cross-section of the electrode. The electric current density is measured in amperes per square meter (A/m^2). It is a vector quantity whose magnitude depends on current per cross-sectional area. It is represented as follows:

Current Density (J) = $\dfrac{\text{Total flow of charge per time (in Amp.)}}{\text{Cross sectional area (m}^2\text{)}}$
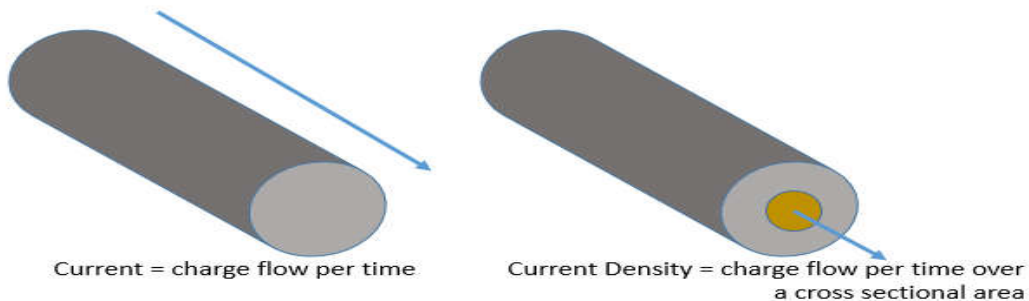
Fig 2.2 Electric current I (left) and current density J (right).

The current density is an important measuring parameter to compare the current produced by two different fuel cells. Because cell performance depends strongly upon the current

produced, and the current density then is determined by the cross sectional area of the conducting elements.

Power Density: It is ratio of power generated by the cell to the specific surface area of electrode. Sometimes it is called as specific power and in SI it is represented in W/m^2.

$$\text{Power density = current density x voltage of cell}$$

2.3 Electrical conductance and conductivity

The inverse of electrical resistance of an electrical conductor is called electrical conductance. It is a measure of ease to pass the current through the conductor. Its unit is Siemens (S).

$$G = \frac{I}{V} = \frac{1}{R} \text{ , where } R = \frac{V}{I}$$

The slope of I vs V curve in linear sweep voltammetry, gives conductance G.

Electrical conductivity (σ): Also called as specific conductance. It is the ability of the material to conduct the electric current and is reciprocal of resistivity (ρ). SI unit is S/m.

$$\sigma = \frac{1}{\rho} \qquad \rho = R\frac{l}{A} \qquad \sigma = \frac{l}{RA} = \frac{Gl}{A}$$

R=electrical resistance, *l*=length of the piece of object, *A=A*cross-sectional area

2.4 Overpotential and crossover

Overpotential: The term directly relates to the efficiency of voltage. It is the extra potential required to re-establish equilibrium for a redox reaction [6] [7].

As the current density increases, overpotential also increases and is described by the Tafel equation. Tafel equation for an electrode is given by [6]:

(13)

$$\Delta V = A \times \ln(\frac{i}{i_\circ})$$

Tafel plot for anodic reaction [6].

* ❖ ΔV or η(v) is the overpotential,
* ❖ A = "Tafel slope", V
* ❖ i = current density, A/m^2
* ❖ $i_\circ$ = exchange current density, A/m^2. The exchange current density is the current in the non-appearance of net electrolysis and at nil overpotential.
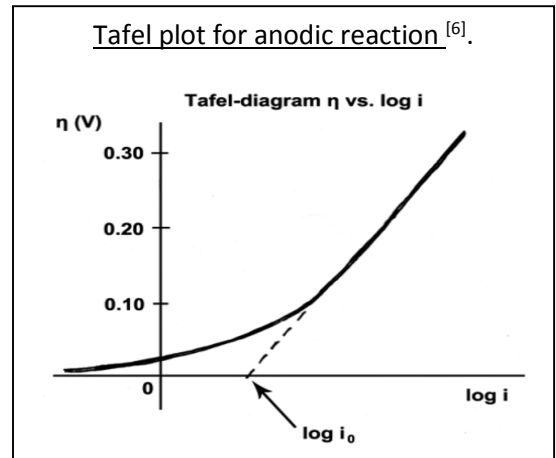
Assumption: Reverse reaction rate is negligible compared to the forward reaction rate.

At Higher polarization values Tafel equation is applicable but at lower value of polarization, current dependence on polarization is linear i.e. ohmic behavior. Then:

$$i = i_\circ \frac{nF}{RT} \Delta E$$

Types of overpotential:

1) Activation overpotential: This refers to the activation energy which is required to transfer an electron from the electrode to the electrolyte. Also called as electron transfer overpotential. The reaction overpotential falls in this category, the activation overpotential required to carry out a chemical reaction in cell. The electrolyte and the electro-catalyst can reduce the reaction overpotential.

2) Concentration overpotential: It is overpotential due to loss of charge-carriers at the electrode surface. Diffusion and Bubble overpotentials fall under concentration overpotentials. Slow diffusion rate is responsible for concentration diffusive overpotential and generation of bubbles due to evolution of gases at either of the two electrodes and the resulting depletion of charge-carriers leads to bubble overpotential [7].

3) Resistance overpotential: This overpotential is produced due to cell design and connections of the cell. Junction overpotential occurs at electrode surface and electrolyte.

<u>Crossover</u>: Unwanted mixing and transport of fuel and oxidant at undesired electrodes leading to unwanted secondary reactions. This degrades the OCV and effects the overall performance.

2.5 Three electrode system

Three basic electrodes and their functions are as follows:

<u>Working electrode</u>: The electrode in electrochemical system at which interest of reaction takes place. This electrode is always in combination with counter and reference electrodes in a three electrode system. Depends on the nature of the reaction at the electrode i.e., oxidation or reduction, it is called anode or cathodey.

<u>Auxiliary electrode</u>: This electrode is also called as counter electrode. In three electrode system, current is expected to flow into it. This electrode establish counter potential with respect to working electrode. Generally, The auxiliary electrode has a larger surface area than working electrode to establish the half-reaction occur fast enough at auxiliary electrode, so it not limit the process at the working electrode.

In a *two-electrode system*, one of either current or potential is previously set amongst the working and auxiliary electrodes, so other variable could be measured.

<u>Reference electrode</u>: This electrode has established and well familiar potential with high stability that is commonly approached by set down a redox system which contains buffered or saturated concentrated solution of every reactant present in the redox reaction.
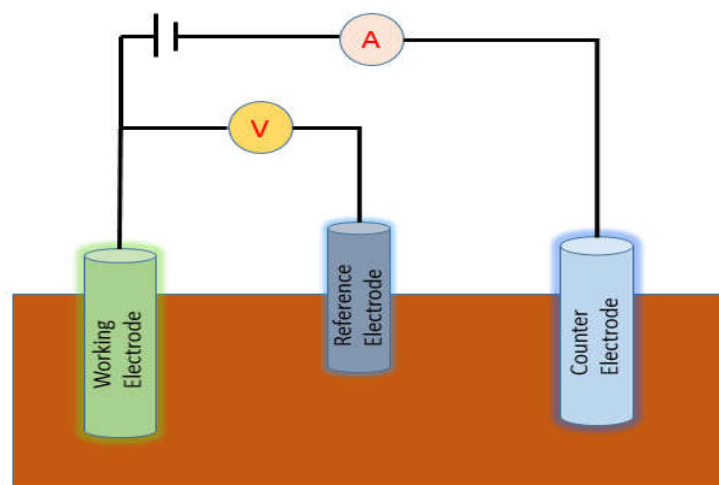
Fig 2.5 Three electrode system representation

2.6 Fuel & oxidant and cell losses

Fuel: Any chemical or material that can be easily react and releases chemical or nuclear energy which can be used to generate power. In fuel cells, fuels are oxidized in the redox reaction at the anode and produce electricity for work.

Oxidant: A chemical substance that oxidizes another substance in a redox reaction. Oxidant is a chemical solution which transfers electronegative species, often oxygen, to another chemical substance. Ex- H_2O_2, $KMnO_4$ etc.

Losses of cell:

 Losses: can be divided into fuel crossover and internal currents, mass transport, activation, ohmic losses. These are the reasons for the real OCV to be lower than the theoretical OCV.
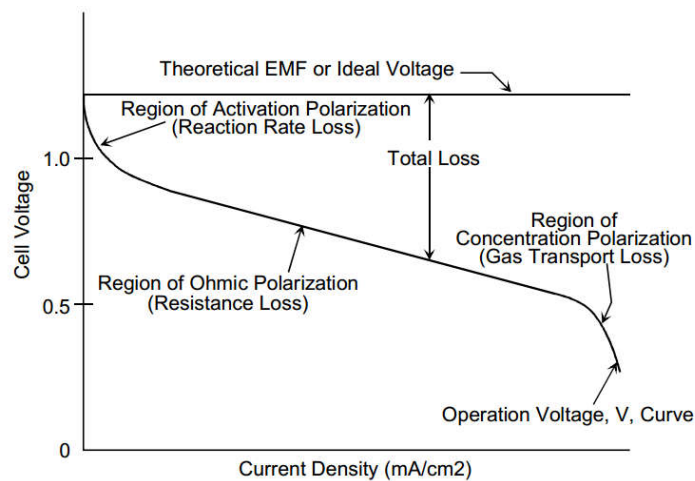
Fig 2.6 Representation of losses of cell using Voltage vs Current density curve [6]

1) Activation loss: Due to slowness of reaction (reaction kinetics) taking place at the electrode surface, causes voltage decrease.

2) Ohmic loss: Hindrance in the drift of ions into the electrolyte and electrons due to connection setup through the cell assembly, causes voltage drop.

3) Mass transport loss: Decease in the concentration of reactants at electrode surface as fuel is used, decrease in voltage, as reactants are consumed, soon the fuel should supplied.

Chapter 3

Instruments and characterization techniques

Instruments and characterization techniques

3.1 Autolab metrohm instrument

This instrument is used for electrochemical measurements and works with Nova software.

Benefits of instrument:

1) Wide range of organic and inorganic samples can undergo the experiment.

2) Since the techniques are advanced, therefore lack of contamination.

3) In open glassware experimental configuration, this allows injection of the solution directly to the sensor surface, can see the change in results immediately.

4) Instrument is very sensitive, voltage range mV to 10 V and current range microampere to milliampere, biological sample also can be analyzed.

3.1.1 Chronopotentiometry and chronoamperometry

Chronopotentiometry

An electrochemical analysis in which the rate of change of potential at an electrode is measured at constant set current. Autolab Metrohm instrument is capable of both a potentiostat (controlled potential) and a galvanostat (controlled current) experiments. However potentiostatic experimental setups are much more regular than the galvanostat. Sometimes galvanostatic modes are advantageous. In potentiometric striping analysis with constant current measurements, solution resistance causes the ohmic drop in voltage usually stays constant with respect to fuel concentration, as resulting voltage is equal to the product of the current and the resistance caused by solution. It also provides data to monitor stability of cell voltage with time. Fig 3.1.1 (a) referred for the chronopotentiometric setup operated with the Nova software and result output comes as potential vs time curve.

Remarks   Chrono potentiometry (Δt > 1 ms)
End status Autolab
Signal sampler   Time, WE(1).Current, WE(1).Potential
Instrument description
⊞ Autolab control
⊞ Set current   0.000E+00
⊞ Set cell   On
⊟ Wait time (s)   5
    Duration (s)   5
⊟ Record signals (>1 ms) galvanost.. [5, 0.01]
    Duration (s)   5
    Interval time (s)   0.01
    Estimated number of points 500
    Signal sampler   Time, WE(1).Current, WE(1).Potential
    Options   No Options
    Use fast options   No
    Corrected time   <.array..> (s)
    Time   <.array..> (s)
    WE(1).Potential   <.array..> (V)
    WE(1).Current   <.array..> (A)
    Index   <.array..>
  ⊞ E vs t
⊞ Set current   5.000E-04
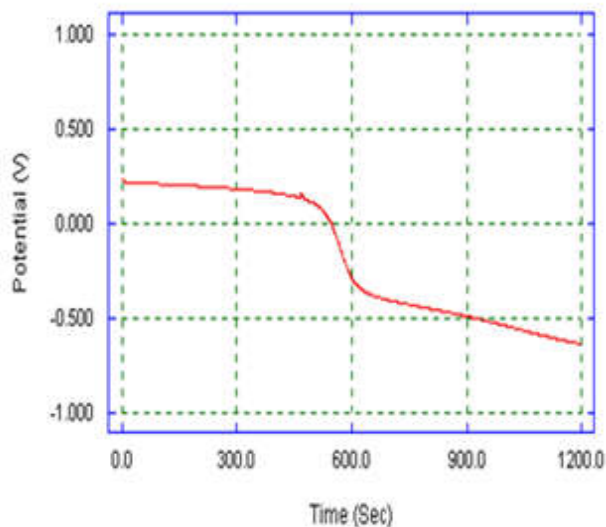
Fig 3.1.1 (a) Chronopotentiometry setup in Nova software (left) and output curve V vs Time (right)

Chronoamperometry

In this electrochemical experiment, the current is measured with respect to the time at set potential. This setup is almost similar to chronoamperometry but it gives current vs time curve at set potential, tells how much time is current of cell is stable and after what time they are going be diminished.

Chrono amperometry (Δt > 1 ms)
    Remarks   Chrono amperometry (Δt > 1 ms)
    Options   1 Options
    Instrument
    Instrument description
⊞ Autolab control
⊞ Set potential   0.000
⊞ Set cell   On
⊞ Wait time (s)   5
⊟ Record signals (>1 ms)   [5, 0.01]
    Duration (s)   5
    Interval time (s)   0.01
    Estimated number of points 500
    Signal sampler   Time, WE(1).Potential, WE(1).Current
    Options   1 Options
    Use fast options   No
    Corrected time   <.array..> (s)
    Time   <.array..> (s)
    WE(1).Potential   <.array..> (V)
    WE(1).Current   <.array..> (A)
    Index   <.array..>
  ⊞ i vs t
⊞ Set potential   0.500
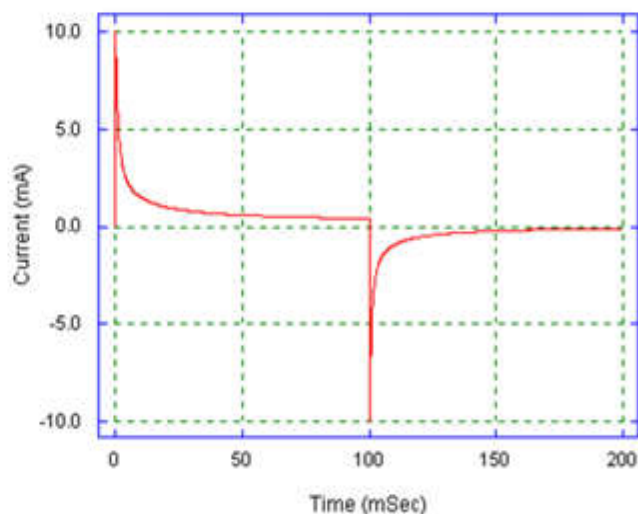
Fig 3.1.1(b) Chronoamperometry setup in Nova software (left) and Output curve Current (*I*) vs Time (right)

3.1.2 LSV: Linear Sweep Voltammetry

In voltammetry, analyte information is procured by determining the current as the act of varied potential. This voltammetry is comes under one of the voltammetric methods into which the current is studied on a working electrode even if the potential amidst the working electrode and auxiliary electrode is swept linearly in time. A peak maximum is registered for oxidation or reduction of species and trough for the variant molecules commence to get either oxidized or reduced during current signal at the respective set potential.
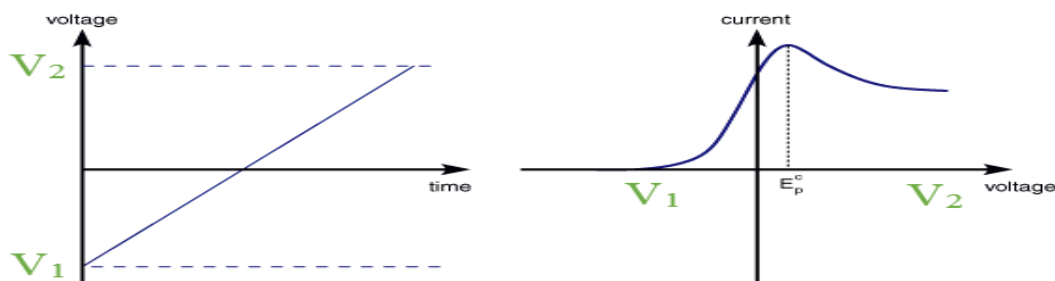
Fig 3.1.2 Linear sweep voltammetry. V vs time and V vs I graph

These are simply potential step measurements in which a fixed potential is employed. Here the voltage is scanned from lower to upper limit of set voltage. The scan starts from V_1 voltage where no current flows. As the voltage increase further towards the V_2 voltage, the current begins to flow and ultimately reaches a peak before dropping. $E_p^°$ is the voltage where the current is maximum.

3.1.3 Electrochemical Impedance Spectroscopy (EIS)

Electrochemical Impedance Spectroscopy (EIS) is a unique characterization technique to deduce the charge transfer and transport mechanisms in electrochemical cells. There are three elemental issues which causes voltage loss in fuel cells: (1) Kinetic or activation losses due to charge transfer polarizations,(2) Ohmic losses due to hindrance to flow of ions within electrolyte, and (3) Mass transport losses due to decrease in reactant concentration over the electrode surface. EIS spectroscopy technique is adequately competent to quantify, detect and separately interpret theses sources of Impedance or polarizations present in the fuel cell. By this spectroscopy we can easily extract out worthwhile analysis with measurable information regarding the sources of resistances within the particular fuel cell. With the help of interpreted curves implementation of physically-sound equivalent circuit models produced wherein a

network of inductors, resistors and capacitors represents physiochemical processes events within the fuel cell [8]. EIS is helpful for investigation and growth of new materials and electrode structures to know the losses contained by the system.

It depends on basic principle of interaction of an electric dipole moment of specimen and external field, generally express by permittivity. This system of working acknowledge the impedance within a range of set frequencies, in combination with the energy storage and dissipation properties. EIS data are generally express as curves in two type of plots, (1) Bode plot and (2) Nyquist plot [9].

Bode plot	Nyquist plot
Individual charge transfer process can be resolve	Individual charge transfer process can be resolve
Frequency is explicit.	Frequency is not obvious.
Small impedance in presence of large impedance can be identified easily.	Small impedance can be submerged by large impedance.
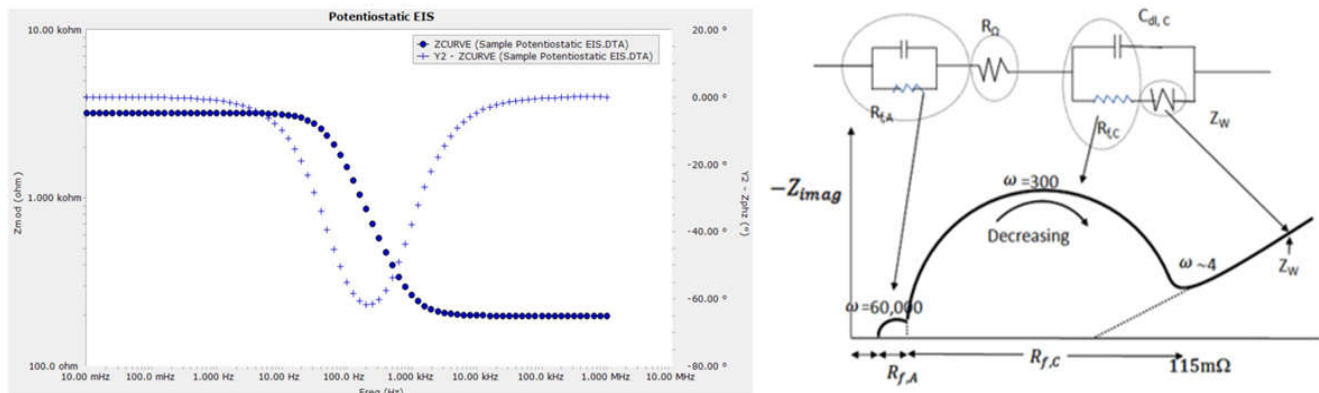
Fig 3.1.3 Bode Modulus and phase plot (left) and Nyquist plot (right) [9]

3.2 UV-Visible spectroscopy

It is absorption and scattering spectroscopy in UV-Visible region. Chemical compound having π-electrons or non-bonding electrons (n-electrons) can easily absorb the energy given by light in UV-Visible range and electrons get excited from lower orbital to higher anti-bonding molecular orbital. More easily the electrons get excited means lesser amount of energy required causing lowering in the energy gap between the HOMO and the LUMO orbitals, the longer will be the

wavelength of light it can absorb. Dilute solution samples are used for this spectroscopy. This also very useful in primary detection of nanoparticles, whose Plasmon peak comes in UV-Visible range.
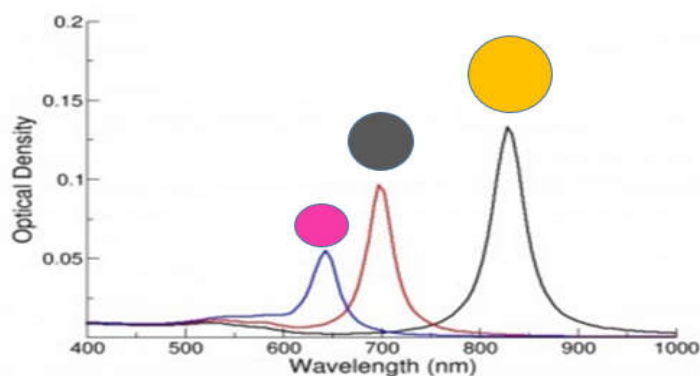
Fig 3.2 Particle with different size shows different Plasmon peaks in UV-Visible spectra

Metal nanoparticles of gold, silver, and platinum which have efficient tendency for absorption and scattering of light, shows a plasmatic peak in UV-Visible range. The optical property of nanoparticles are tunable which changes with change in size, change in shape and with different surface coating materials, thereby plasmatic peak also changes or shifts to near-infrared regions from ultraviolet region by passing over visible electromagnetic spectrum. The changes comes in optical property due to shifting the absorption and scattering energy with change in physical dimensions of nanoparticle, chemical nature or reactivity and color of nanoparticle also gets change [10].

Example: Spherical nanoparticles solution of gold (Au) are light red or pink in color due to absorption energy corresponds to green color of the visible spectrum. However Ag-nanoparticles yellowish in color due to corresponding absorption energy comes in the blue region of the spectrum.

3.3 X-Ray Fluorescence Spectroscopy (XRF)

It is a non-destructive analytical technique applied for the determination of the elemental composition of the sample material [11]. XRF detector determines the chemical samples by detecting fluorescent secondary x-rays comes out from the sample when sample is already excited by primarily x-ray source. Every element present in sample produces its own characteristic fluorescent x-ray that is familiar for that element only. That's why XRF spectroscopy is an excellent technique for quantitative detection and elemental analysis of material.
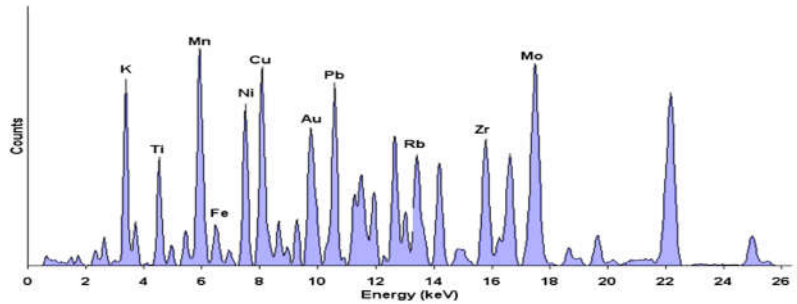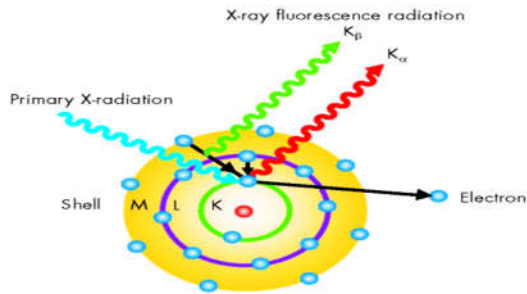
Advantages:

1) Can be used for bulk chemical analyses of number of elements at a time (Na, Ti, Zn, Si, Fe, Mg, Pb, Al, P etc.), present in sample. 2) Bulk chemical analyses of major elements as well as trace elements (<1ppm), present in sample.

Disadvantages:

1) XRF detector cannot recognize ions and element having different oxidation number.

2) Technique is less competent to absolutely and purely determine the plenty of elements with atomic number lower than sodium. Helium gas is required for ppm level detection of sodium.

3.4 SEM-Scanning Electron Microscopy

In scanning electron microscope, a totalize beam of high-energy electrons falls at the surface of solid specimens to produce a variety of signals. The signals generated by interactions of electron beam and sample surface reveals the information about texture, chemical composition & orientation and crystallinity of material. The SEM is used to create high-resolution image to see shapes, spatial variations and chemical compositions of the sample, which cannot be done by optical microscope.

SEM technique can take image with tunable magnification ranging from 20x to 25000x with masterly resolution of 50 to 100 nm.

Advantage: (1) The versatile information: detailed three-dimensional and topographical imaging. (2) This instrument works fast.

Disadvantage: (1) Only solid samples can be analysed easily which must be small to put in the vacuum chamber. (2) SEMs are expensive and sensitive to electromagnetic radiations.

Chapter 4

Introduction of
paper based fuel cell

Introduction of paper based fuel cells

Paper Based fuel cells are designed such, that the catholyte and anolyte run separately and undergo electrochemical reactions, as a result of laminar flow of reactants on porous paper. Capillarity is one of the major functionality of fluids on porous paper which provides the impetus to work on this newly assembled deign of fuel cell i.e., Paper based fuel cell.

This cell can be used for diagnostic purposes such as biological samples. Since paper turns wet after a few minutes causing degradation of paper, so in consequence these cells have a short life time and thus can be used only for short duration operations like paper based diagnostic strip machine for glucose in blood, urea in urine and digital pregnancy test machine etc. The advantages of paper based fuel cells include quick disposability, flexibility, thin and small assembly configuration, and its ability to serve as a portable device [5] [12] [13].

4.1 Recent literature

A self-pumping and autonomous-breathing paper based fuel cell with stroked pencil on paper used as graphite electrodes [12]:
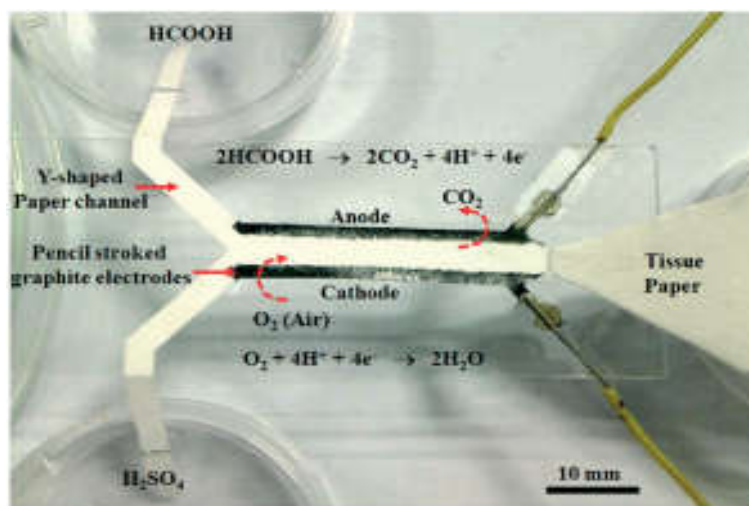
Fig 4.1 (a) Paper-based fuel cell with using graphite electrodes made by stroking Hb-pencil on paper to demonstrate an autonomous-pumping and air-breathing fuel cell [12].

In this paper, authors created a paper based fuel cell in which the fuel (formic acid) flows due to a capillarity transport contrivance. In this cell, formic acid is fed as a fuel and sulfuric acid serves as the oxidant.

In this paper, authors have designed an innovative and easily operative paper-based membraneless fuel cell that operates without any pumping system. Graphite porous electrode were fabricated with the rubbing of an Hb-pencil on Whatman filter paper and number of rubbed pencil stroked namely K were created.

Key points about this literature:

- ❖ Fluids flow through a capillary action.
- ❖ Fuel: HCOOH (1 M), oxidant: H_2SO_4 (3.75 M) with ambient air.
- ❖ Maximum OCV = 0.33 V, which dropped to 0.27 V (after some time).
- ❖ Power Density = 32 mW/cm^2, for 1000 minutes.
- ❖ Max. Current density = 660 mA/cm^2.
- ❖ Number of graphite strokes (K) = 35 to 300.
- ❖ At K = 200, OCV = 0.33 V was maximum.

SEM image taken before and after pencil strokes reveals that strokes of the Hb-pencil done over the another strokes allowed the paper fibers to adsorb graphite

layer for regular flat shaped electrodes. But the maximum voltage was obtained at K = 200 strokes and there after the OCV decreased which was attributed to loss in electrode continuity due to increase in resistance of the electrode. At the anode of the open paper fuel cell, liberation of CO_2 gas to the atmosphere occurs.
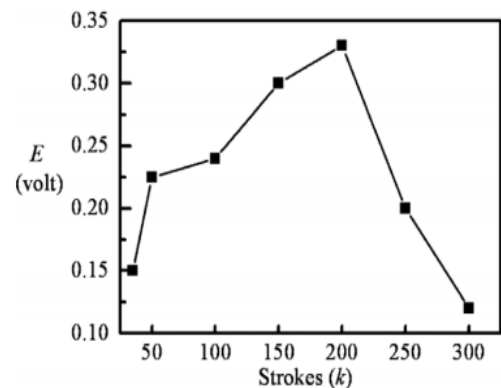
Fig 4.1 (b) Cell OCV as the function of increase number of pencil strokes [12]

**To meet the power needs of next generation, microfluidic fuel cells based on paper support used as lateral flow diagnostic paper strip devices [13]:**

In this paper, the authors developed microfluidic fuel cells which are paper based and the advantage of laminar flow on a porous paper material by capillary action was shown. Paper-based power sources can be thus used as lateral flow test strip diagnostic systems. In their represented design, the two streams flows parallely on porous paper.
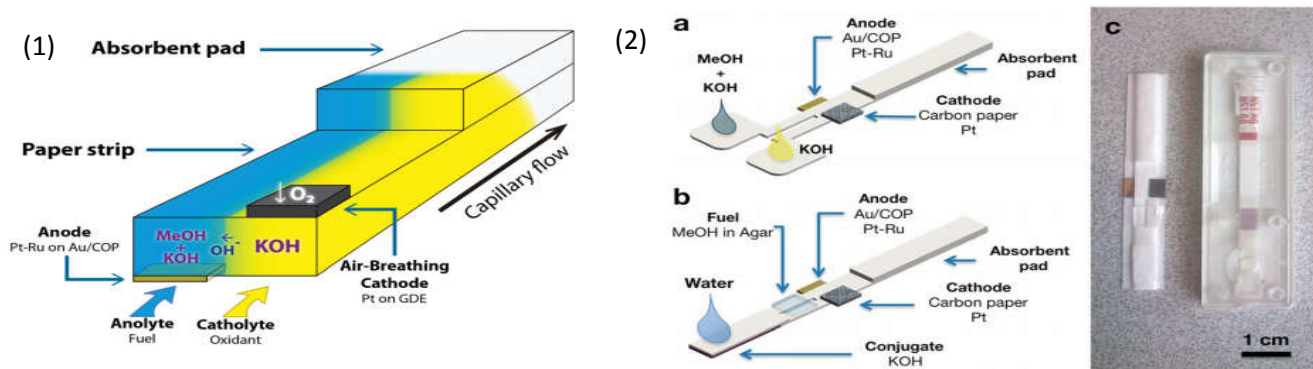
Fig 4.1 (C) Sketchy design of paper based microfluidic fuel cell **(1)**, a paper-based lateral flow test strip fuel Cell **(2a,b)**. Comparison of a paper-based cell with commercial available dengue estimation test strips **(2c)** [13].

The application on a paper strip within the fuel cells allows the flow of fuel without the use of any external pumps. Authors [J. P. Esquivel, F. J. Del Campo, J. L. Gomez de la Fuente, S. Rojas and N. Sabate] showed storage of KOH electrolyte in a solid form by the use of a conjugate and a methanol-rich agar gel piece kept over top of the reaction pathway which allows this cell to work by soaking the sample pad with just water. At anode, an Au-catalyst used on composite-PtRu and Pt/carbon paper at cathode worked as an air breathing electrode. In Fig 4.1 (C) (**2b**, *Right*), the agar gel piece enriched by MeOH stored MeOH for further use and this piece is placed over the slit. To prevent the catholyte stream from diffusion of MeOH present in the agar gel, the cathode side was laminated before use. When a drop of the water fed to the cell, the KOH in conjugate pad dissolves and flows towards the slit where at the anolyte side, MeOH extrudes from the agar gel and only KOH passes through the catholyte side because of lamination. The cathode is fed with only KOH with ambient air present therein. Thus, KOH is sufficient as an electrolyte to maintain the ion transport between electrodes and completes the cell [13].

Key features:

- ❖ Fuel: Methanol
- ❖ Electrolyte: KOH
- ❖ Anode: Au/ composite Pt-Ru
- ❖ Cathode: Carbon paper/ Pt
- ❖ Catalyst loading: 1 mg/cm^2 of the total metal load on electrode surface
- ❖ Anolyte: Methanol and KOH, Catholyte: KOH

- ❖ Max. Power Density = 4.4 mW/cm^2

  Max. Current density = 22.5 mA/cm^2

  Obtained at 4 M methanol (optimum Fuel concentration) and 2 M KOH (optimum electrolyte concentration) [13].

By this paper, they provided the idea of storing of both the KOH electrolyte and the methanol fuel by using an agar gel. The cell works with a small amount of water. The individual electrochemical features of the fuel cells make it competent for producing stable power and fulfilling the needs to compute the results of rapid flow diagnosis tests.

4.2 Objectives of the work

❖ Fabrication of a paper based fuel cell of a suitable geometry which is light weight and capable of delivering power density in micro-nano range for short time operations.

❖ Obtaining OCV and power density greater than 1 V and 1 mW/cm^2 respectively, at room temperature.

❖ Characterization of the fuel cell systems by chronopotentiometry, chronoamperometry and EIS measurements.

❖ Application of acidic and alkaline gel membrane as electrolytes in the different fuel cell systems.

❖ Synthesis of suitable catalysts and their implementation on the cell.

❖ Characterization of as in the cells prepared catalyst and electrolytic gels.

❖ Impedance studies of the T-shaped cell.

4.3 Advantages of paper based fuel cells

❖ Low-cost, lightweight and compact, portable and ability to yield fast results.

❖ Significantly simpler working and ease of fabrication.

❖ Paper-based microfluidic fuel cells are useful for numerous short time electrical applications.

❖ The fluid flow rates have been found to be very low, and can be stabilized by use of absorbent pads, and consequently a less amount of fluid can be delivered for a long period of time.

❖ These cell do not require the pumping of solutions / gases.

❖ The cells can be operated at room temperature.

Chapter 5

Fabrication of cell and its components

Fabrication of cell and its components

In this work the fabrication of cell was done by using two inverted L-shaped paper strips (*Whatman filter paper, CAT No. 1440-150*) and by maintaining a constant spacing between them (0.2 cm) till the strips reach the absorbent pad made up of tissue paper as shown in Fig 5.1 (a). The width of the two strips was kept same and each strip was dipped in a solution of either fuel or oxidant kept in the petri-dishes. The gel electrolyte was placed in between these two strips and the electrodes were kept over the respective anolye and catholyte paper strips.

This assembly was always first fed with a small amount of fuel or oxidant prior to the experiment and then due to the porosity of the Whatman filter paper and the capillary action of the fluids on the porous paper, the anolyte and catholyte streams runs parallel, without any external pumping device. This is the cell assembly and it works as a self-pumping system where fluids are kept in petri-dishes (as reservoirs). We have fabricated the cell by using a glass slide for supporting the Whatman filter paper strips, two petri dishes, connecting wires and normal tissue paper. Thus this fabrication of this fuel cell assembly is simple, facile and it is very easy to re-generate the cell in very less time.

5.1 Appearance at a glance of the cell assembly
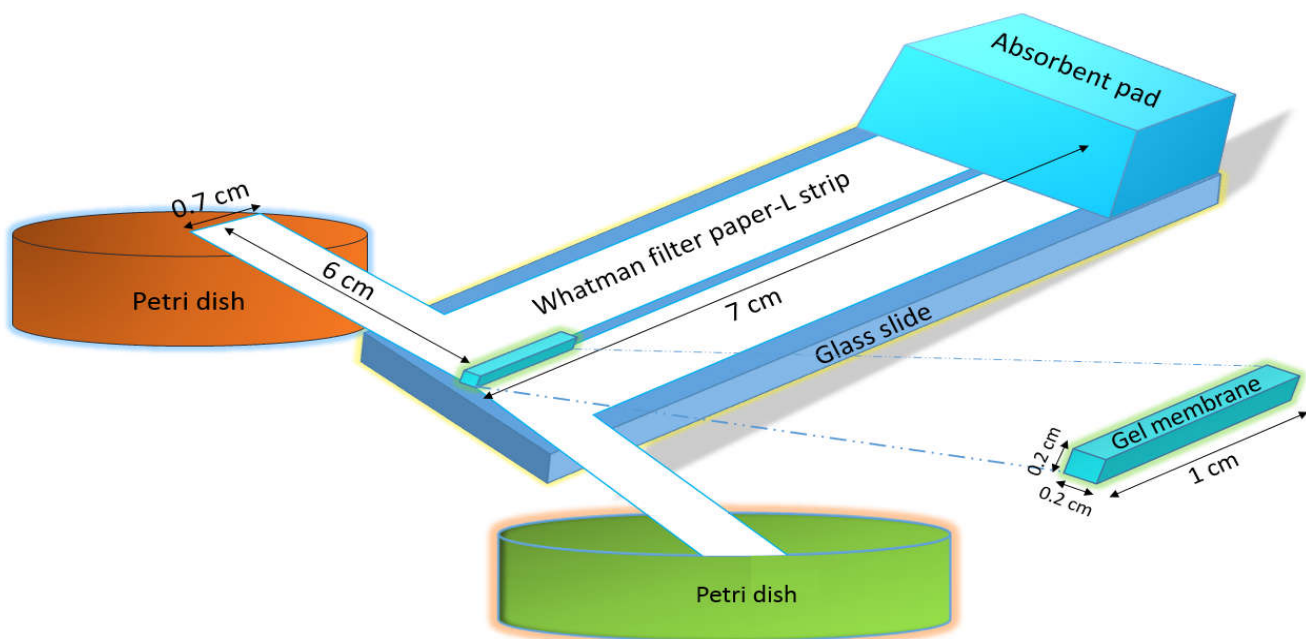
Fig 5.1(a) Representation of T-shaped paper based fuel cell with a gel electrolyte.

There are different dimensions of the same strip in cell and these can be seen in Fig 5.1(b). The cell setup by uses two L-shaped Whatman filter paper strips and these placed on the glass slide such that the spacing between two the inverted strips stays 0.2 cm and the strips never touch each other. The idea behind keeping the longitudinal portion of strip width at 1 cm which is more than the horizontal width i.e., 0.7 cm, is that when the fluids will come through the horizontal portion of the strip, they have access to more surface area while coming in contact the electrode and the excess finally flows to an absorbent pad.

Fig 5.1(b) T-shaped configuration of cell using two L-shaped inverted

By the continuous supply of fluids, the electrochemical reaction occurs and the byproducts will flow towards the absorbent pad. The absorbent pad absorbs the excessive fuel-oxidant and the byproducts of the reaction, and helps in maintaining the laminar flow of fluids on paper.

In a T-shaped assembly (*shown in fig 5.1(b)*), the gel electrolyte is applied in between the strips at the T-junction and then the graphite electrodes were placed on both strips along using crocodile clips and connected to the PSTAT. 2-3 drops of fuel and oxidant were delivered on the two different strips of paper and the strips were dipped into respective fuel and oxidant solutions to keep constant supply of fuel and oxidant for the cell, as shown in fig 5.1 (c).

Fig 5.1 (c) Image of working cell taken to show the actual setup.

The complete electrical circuit of the T-shaped cell can be represented [fig 5.1 (d)], where the oxidation reaction of the *sodium percarbonate fuel* takes place at the working electrode or anode. Electrons are released at anode and these electrons travel through the external circuit to reach the cathode where the reduction reaction of *potassium permanganate* oxidant takes place. The gel electrolyte helps in ion transport between the cathode and anode, and completes the electrical circuit. The depleted fuel/oxidant solutions along with the byproducts generated after the reactions at anode/cathode respectively flow to along the porous paper strips, and ultimately reach the absorbent pad which can soak up large amount of fluids.
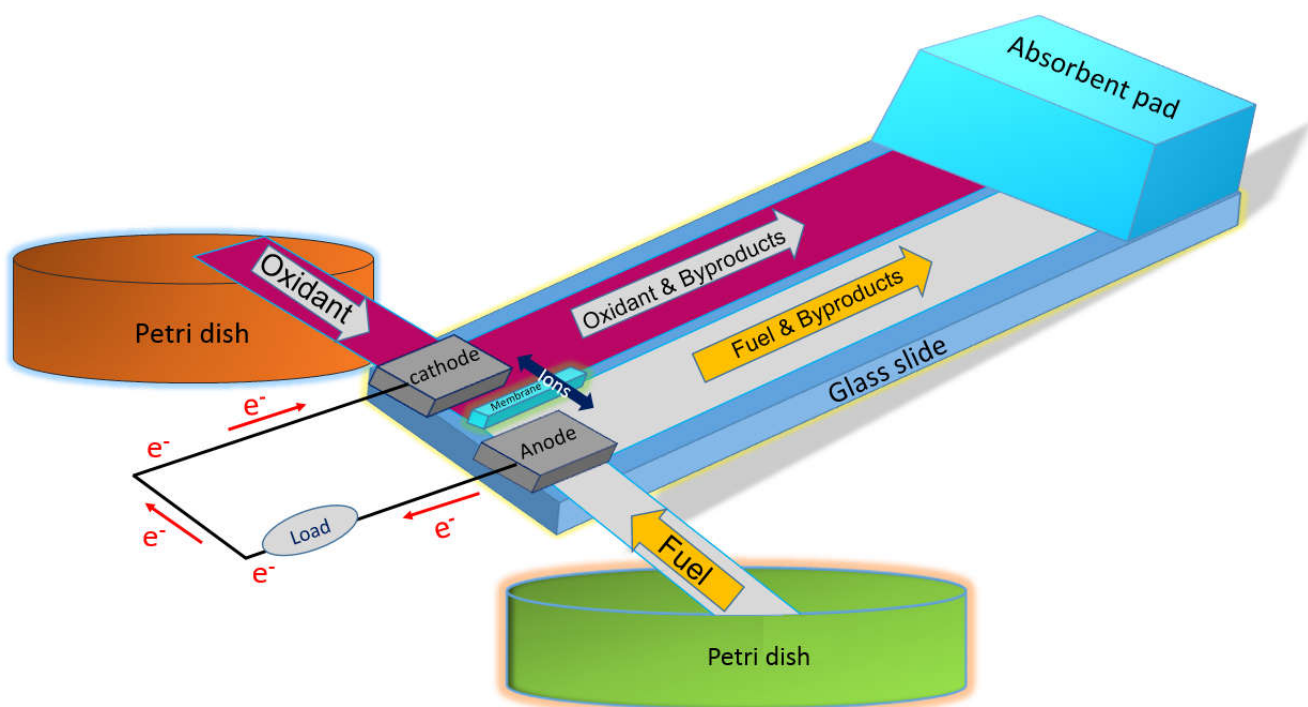
Fig 5.1 (d) Representation of the complete electrical circuit for T-shaped paper based fuel cell.

The petri dishes contain the fuel or oxidant solutions and functions as reservoirs of fuel or oxidant where the porous paper strip is dipped. Dipped strips due to capillary force of fluid on the porous paper, ensures the fuel or oxidant supply to the electrodes. This feature makes it a self-pumping fuel cell.

5.2 Gel electrolyte preparation

In this project, two types of gel are prepared. Both gels were applied at the junction of strips. Preparation of gel membrane involves two steps. The first step is same for the preparation of both gels but the second one is different.

Preparation [15]:

Step 1: 1 g of acryl amide was taken in a beaker and 5 mL of deionized-water was   poured into the beaker. The solution was stirred and heated at 90°C at 600 rpm. After heating for 10 mins, 3 mg of ammonium persulfate (source of free radicals and a stabilizer to initiate polymerization) in 1 mL deionized-water solution was poured into the beaker with vigorous stirring, and heated for more 10 more minutes.

Step 2: For acidic gel electrolyte:

2 mL of 2 M sulfuric acid solution was poured into gel and stirred again at 600 rpm for 5 mins without heating.

For alkaline gel electrolyte:

2 mL of 2 M sodium hydroxide solution was poured into gel and stirred again at 600 rpm for 5 mins without heating.

Functions:

1) Acidic gel electrolyte: generally works as a Proton/cation exchange membrane.

2) Alkaline gel membrane: usually works as an anion exchange membrane.

5.3 Electrode used: Graphite but why?

Among electrodes of molybdenum, graphite, tin oxide, copper and platinum, molybdenum and copper are the most popular [16]. Recently compared to the other electrodes, graphite electrodes are attractive due to the following advantages:

1) It is an economical electrode: Low cost (*The cost of graphite electrodes cost ten times lesser than that of molybdenum electrodes [16].*)

2) Lower density and higher porosity

3) Chemical inertness

4) Durable and can used from low to high temperature operations.

5) Good electrical and thermal conductivity enables them to work as excellent current collectors [17].

6) High temperature stability

7) Low thermal expansion

Chapter 6

About present work: Experiments and analysis

About present work: Experiments and analysis

In this chapter we will discuss about experiments on the T-shaped paper based cell with different fuel and oxidant combinations, fuel cell stability with time and temperature, OCV etc.

6.1 Choice of a good fuel and oxidant

It is know that the best fuel is hydrogen which has the highest energy density. But it is not easy to use hydrogen gas for all applications due to its' high calorific value. So, in fuel cells, we use a fuel which gives H^+ in the electrolyte solution (*in PEMFC*) and these protons are transferred from the anode side to the cathode side, which completes the electrical circuit and generates water as product at the cathode side after reacting with the oxidant. Similar is the case for other fuels which generates any anion or cation in solution, and the ions are transferred to the other electrode. Electrons travel from the anode to the cathode and ions movement between the cathode and anode completes the circuit. Hence, we can choose fuel-oxidant combinations on the basis of lower pKa, for acids like formic acid, oxalic acid etc. as fuel, and oxidants like perchlorates, peroxides and permanganates. For a given fuel-oxidant combination, the overall E°_{cell} must be a positive quantity.

Example: Boric acid in an acidic electrolyte as a fuel cannot be oxidized with acidic $KMnO_4$ because the boron in boric acid has +3 oxidation state which is highest oxidation state for boron.

$$B(OH)_3 \longrightarrow BH_4$$
$$\quad (+3) \qquad\qquad\qquad (+3)$$
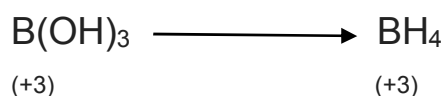
6.2 Different fuel and oxidant combinations attempted

Some of the fuel and oxidant combinations attempted on the T-shaped paper based fuel cell are listed here. Here our aim was to obtain a high OCV, so that further studies on the fuel cell can be done. Combinations attempted were:

1) Oxalic acid (1 M)-Fuel, $KMnO_4$ (0.5 M)-Oxidant, Electrolyte- H_2SO_4 (2 M)
2) Formic acid (1 M)-Fuel, H_2O_2 (2 M)-Oxidant, Electrolyte-H_2SO_4 (2 M)
3) Formic acid (1 M)-Fuel, $K_2Cr_2O_7$ (0.5 M)-Oxidant, Electrolyte-H_2SO_4 (2 M)
4) Hydrogen iodide (0.5 M)-Fuel, $KMnO_4$ (0.5 M), Electrolyte-H_2SO_4 (2 M)
5) Sodium Percarbonate (1 M)-Fuel in electrolyte NaOH (1 M), $KMnO_4$ (0.5 M)-oxidant in electrolyte-H_2SO_4 (2 M)
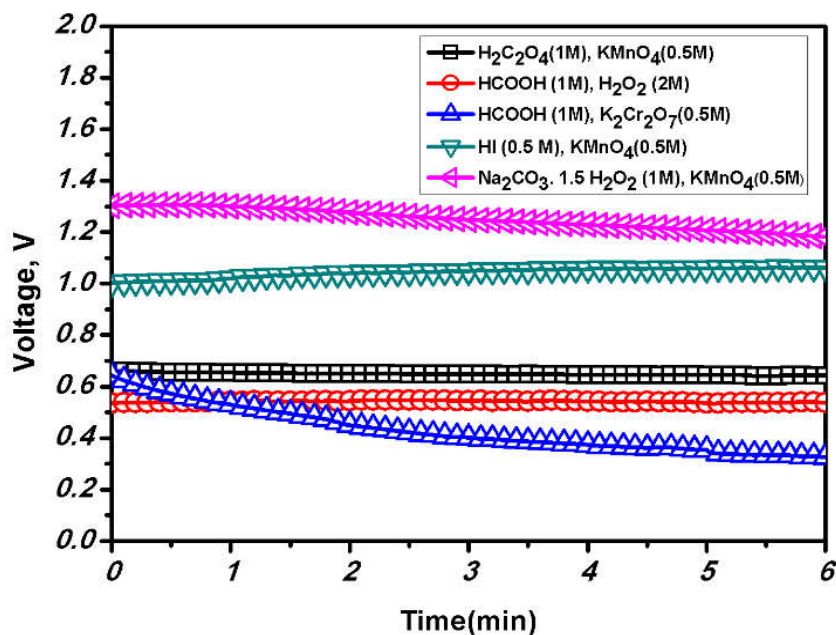
Fig 6.2 Voltage vs time curve for attempted different fuel and oxidant combinations

By using chronopotentiometry mode, the voltage vs time [fig 6.2] plots were recorded, it was observed that the combination of sodium percarbonate and potassium permanganate as fuel and oxidant respectively, gave the highest OCV (more than 1 V) for 6 mins. Hence the compound: $Na_2CO_3.1.5H_2O_2$ was used as fuel in an alkaline electrolyte and $KMnO_4$ was used as an oxidant in an acidic electrolyte for further studies.

6.3 Sodium percarbonate as a fuel & potassium permanganate as an oxidant

Sodium percarbonate ($Na_2CO_3.1.5H_2O_2$) as fuel

❖ It is adduct of sodium carbonate and hydrogen peroxide [14].

$$2Na_2CO_3.3H_2O_2 \rightarrow 2Na_2CO_3 + 3H_2O_2$$

❖ It is basically the source of anhydrous hydrogen peroxide and very pure [18].

❖ Hydrogen peroxide releases water and oxygen in an aqueous solution.

❖ It is also used for making some of eco-friendly cleaning products.

❖ It is non-toxic, biodegradable and environmentally safe [14].

❖ It is non-flammable, non-explosive and cheap.

❖ It is easily soluble in water and easy to carry anywhere. It is not hazardous material [18].

❖ It leaves no harmful by-product or residues which can harm the environment.

These properties of sodium percarbonate make it versatile fuel.

(37)

Potassium permanganate as an oxidant

❖ It is a strong oxidizing agent. It dissolves in water and gives a purple colored solution.

❖ It does not produce toxic-byproduct.

❖ In an acidic medium, it acts as a reducing agent.

$MnO_4^- + 8H^+ + 5e^- \rightarrow Mn^{2+} + 4H_2O$ (l)
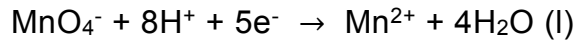
6.4 Open circuit voltage study for different concentration of sodium percarbonate fuel with $KMnO_4$ (0.5M) as oxidant

❖ Fuel (Sodium-percarbonate in basic electrolyte), molar ratio for the fuel and electrolyte kept at 1:1.

$Na_2CO_3.1.5H_2O_2$: NaOH (1:1 molar), (mixed equal volume of fuel and electrolyte for the anolyte solution)

➢ Oxidant (Potassium permanganate In an acidic electrolyte)

$KMnO_4$ (0.5 M) & H_2SO_4 (2 M) (*Fixed*)
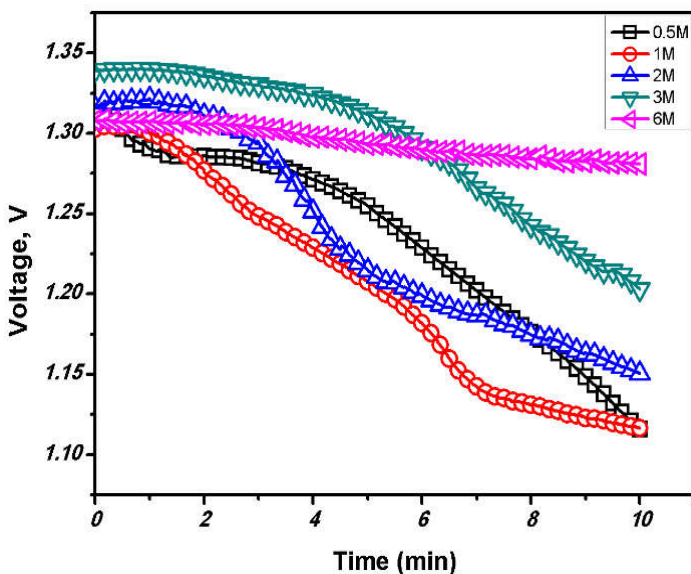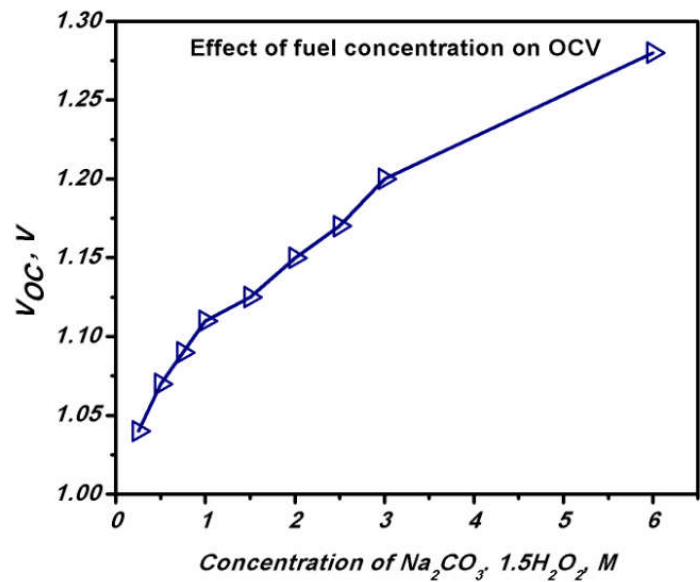
| (a) | (b) |

Fig 6.4 (a) Stability of fuel at different concentration (OCV vs time) and (b) OCV vs concentrations of fuel.

The stability of OCV was determined by using different concentrations of fuel and by plotting OCV vs time. To analyze the voltage drop, cell was run for each concentration for 10 mins

using chronopotentiometry. From the graph [fig 6.4 (a)], It is observed that at 6 M fuel concentration, the performance is best as compared to other concentrations of fuel. But 6 M is not a clear solution, at room temperature. Since, we are seeking cell operation at room temperature, a 3M fuel concentration gave the second best result. The 3M fuel solution is clear and OCV decay is by 0.04 V over 6min; therefore the optimum concentration for fuel is fixed at 3 M sodium percarbonate in 3 M NaOH as an alkaline electrolyte.

We have also plotted OCV versus concentration of fuel. In fig 6.4 (b), even at a minimum concentration (0.25 M) of the tested fuel, the OCV is more than 1 V. On increasing concentration 0.25 M to 1 M, the increase in OCV occurs by 0.07V, but from 1.0 M to 3 M fuel concentration, the OCV increased by only 0.09 V and then from 3M to 6M, it increased by 0.08V. The increase in OCV is much faster in the lower concentration (0.25M to 1M) range than higher concentration range (1 M to 3 M and 3 M to 6 M). This implies that initially OCV increases rapidly due to availability of more fuel and in the higher concentration region, any more increase in concentration does not increase OCV much.

Chapter 7

Different electrolyte and different gel electrolyte combinations, catalytic and EIS studies

Different electrolyte and different gel membrane combinations, catalytic and EIS studies

In this chapter, we will discuss three combination of different gel and electrolyte and discuss the polarization curves. We also discuss the catalyst effect on the performance of cell and electrochemical impedance measurements at different fuel concentration for the cell.

For all the experiments, graphite electrodes were used and the active surface area of the electrode that remains in contact with the paper strip is 0.56 cm^2.

7.1 Three combinations used on the T-shaped cell

7.1.1 Acidic Media

In this experiment, all components or chemicals are in an acidic medium.

Fuel: $Na_2CO_3.1.5H_2O_2$ (variable concentration from 0.5 M to 3 M)

Oxidant: $KMnO_4$ (concentration fixed 0.5 M)

Both fuel and oxidant were mixed in equal amounts of *H_2SO_4 as electrolyte* with fixed concentration of 2 M in all acidic media experiments.

Gel electrolyte: An acidic gel electrolyte was used.

Reactions involved:

A solution of sodium percabonate in water gives the following reaction:

$$2Na_2CO_3.3H_2O_2 \text{ (in aq. Solution)} \rightarrow 4Na^+ + 2CO_3^{2-} + 3H_2O_2$$

When the fuel is mixed with a H_2SO_4 (2 M) solution, carbon dioxide is released. CO_3^{2-} ions on anode side will react with the acidic electrolyte or water and give vigorous effervescence due to formation of carbon dioxide as follows:

$$CO_3^{2-} + H_3O^+ \rightarrow HCO^{3-} + H_2O$$
$$HCO^{3-} + H^+ \rightarrow CO_2 + H_2O$$
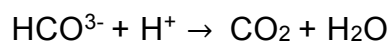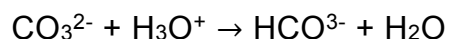
At anode, the oxidation of the fuel (sodium percarbonate) takes place. The aqueous solution is prepared of $2Na_2CO_3.3H_2O_2$. It leaches out H_2O_2. This solution is mixed with an equal amount of acidic electrolyte (H_2SO_4, 2 M). Hydrogen peroxide is a weak acid and in the presence of an acidic electrolyte, it gives 2 proton and 2 electrons.

$$H_2O_2 \rightarrow 2H^+ + O_2 + 2e^-$$
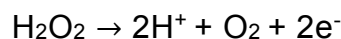
These protons travel through the acidic gel electrolyte from the anode side to the cathode side. And at the cathode side, the electrons from the anode reach the cathode and the reaction of potassium permanganate occurs.

$$MnO_4^- + 8H^+ + 5e^- \rightarrow Mn^{2+} + 4H_2O$$

The following redox reactions is occur in acidic media and their respective electrode potentials are provided below [19].

$MnO_4^- + 8H^+ + 5e^- \rightarrow Mn^{2+} + 4H_2O$	$E^\circ_{red.}= 1.506$ V
$H_2O_2 \rightarrow 2H^+ + O_2 + 2e^-$	$E^\circ_{ox.}= -0.695$ V
$2MnO_4^- + 6H^+ + 5H_2O_2 \rightarrow 2Mn^{2+} + 8H_2O + 5O_2$	$E^\circ_{cell}= 0.812$ V
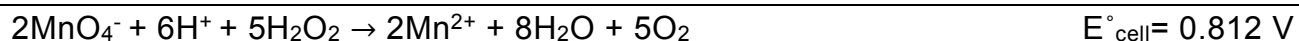
Polarization curves for T-shaped paper based cells in all acidic media
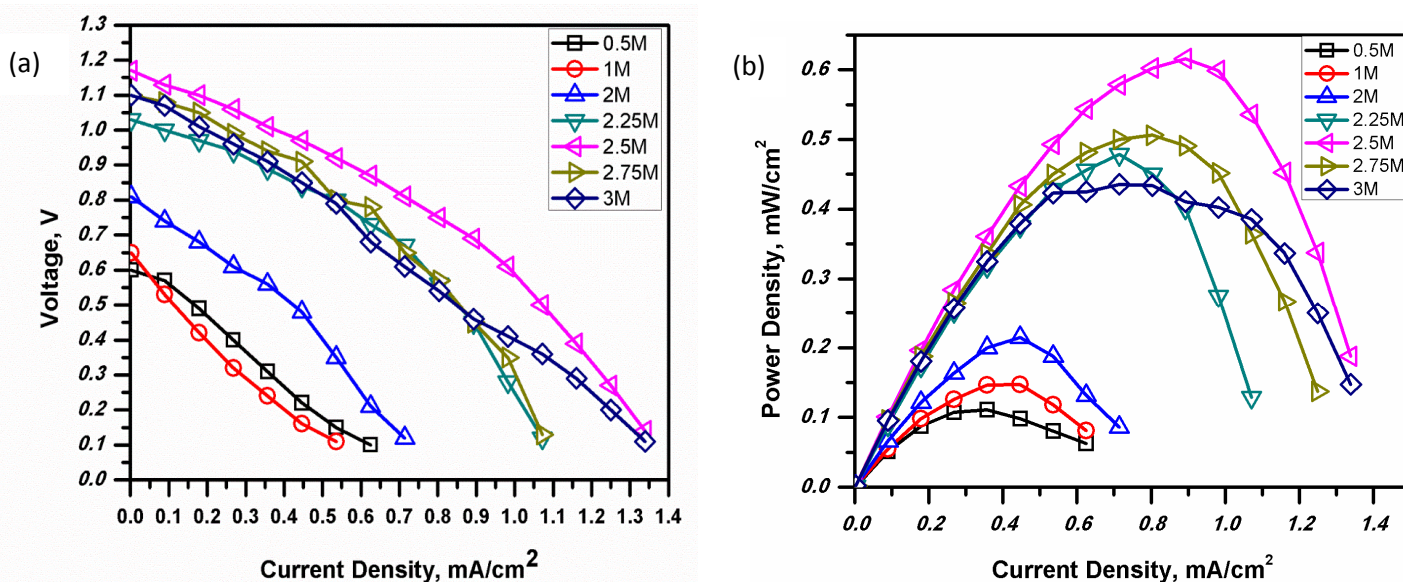
Fig 7.1.1 (a) Voltage vs current density curves with different fuel concentrations and same oxidant concentration. (b) Power density vs current density curves for all acidic media for T-shaped paper based fuel cells.

In this experiment of all acidic media on T-shaped cell assembly, the maximum current density = 1.35 mA/cm^2 and power density = 0.61 mW/cm^2 and these are obtained at 3M fuel concentration. The current density increases with increase of fuel concentration. The current density at 2.5 M fuel is almost three times of the current density at 0.5 M fuel concentration. We obtained an OCV more than the theoretical value i.e., $E°_{cell}$ = 0.812 V. From fig. 7.1.1 (a), at fuel concentration below or equal to 2M, the OCV is within the range of theoretical value. But when the concentration of the fuel is more than 2M, the cell is shows OCV greater than 1 V. The increase in voltage can be calculated with the help of Nernst equation by taking the contribution of Na_2CO_3 along with H_2O_2. At present, we are unable to quantify these concentration terms in the Nernst equation.

From the curves of power density vs current density (Fig 7.1.1 (b)), upon increasing the fuel concentration from 0.5 M to 3 M, the power density first increases up to 0.61 mW/cm^2 at 2.5 M fuel concentration and then decreases with further increase in the concentration of fuel. This is due to the accumulation of carbon dioxide at the anode. Since, the electrolyte H_2SO_4 concentration is fixed, when the concentration of sodium percarbonate fuel is below 2 M or 2.5 M, all the base (Na_2CO_3) present in this adduct (sodium percarbonate) is neutralized by the acidic electrolyte and produces CO_2. But when the concentration is greater than 2.5 M, all the CO_2 produced is liberated from solution by reacting with acidic electrolyte (2M) but some of CO_3^{2-} are present in the solution which are not neutralized by H_2SO_4. Hence extra CO_3^{2-} ions converts to CO_2 via slow reaction with water and cause accumulation at the anode and this results in the decrease of power density with further increase in fuel concentration greater than 2.5 M.

We performed experiments for a 2.5 M fuel concentration, which gave V = 0.9 V at I = 0.3 mA. We cross-checked both current and voltage for 30 mins by using chronopotentiometry and chronoamperometry. We observed that initially the cell generated a voltage of 0.9 V at a set current of 0.3 mA by using chronopotentiometry. But the voltage drops as the time increases till 300 s. At 300 s we again fed the fuel and the oxidant to the system, then the voltage again reached to 0.9 V. This means 0.9 V that current 0.3 mA is reproducible [see fig. 7.1.1 (c)].
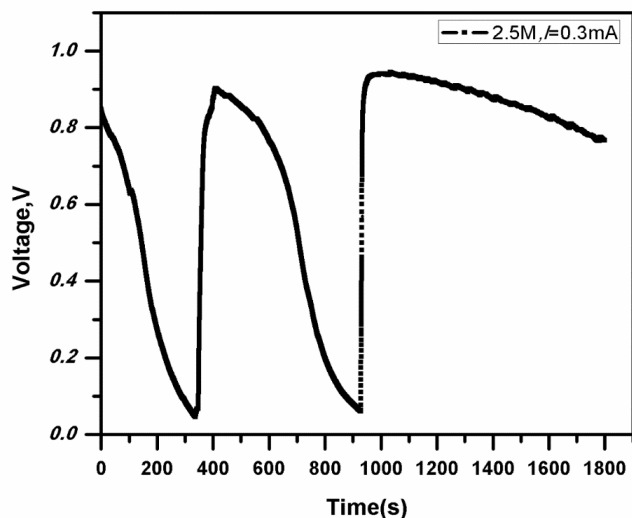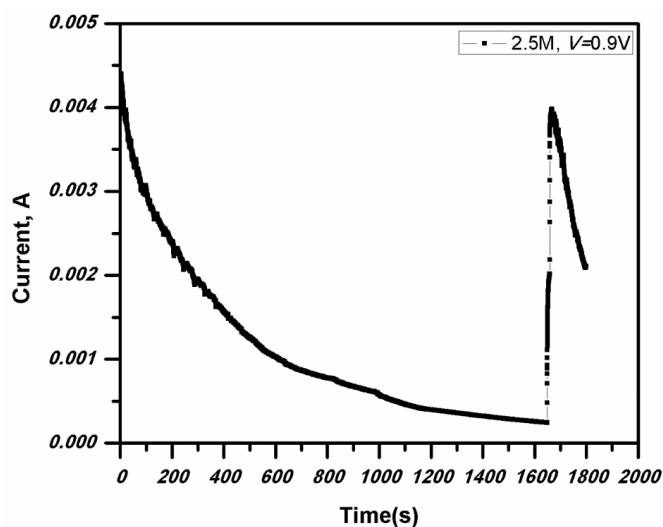
(c)   (d)

Fig 7.1.1 (c) Voltage at a constant current (*I = 0.3 mA*) using 2.5 M fuel, chronopotentiometry run for 3 mins.
(d) Current at constant voltage (V = 0.9 V) using 2.5 M fuel, chronoammperometry run for 30 mins.

Chronamperometry was performed to monitor current at 0.9 V, [see fig. 7.1.1 (d)]. This graph also shows that 0.3 mA current is produced for few seconds at a set voltage of 0.9 V. The current drops to 1 mA within 500 sec, but when the fuel and the oxidant are again fed to the system, it again reaches 4 mA as highest current and able to produce 0.3 mA current easily.

Since sodium percarbonate releases hydrogen peroxide in the solution. Experiment were performed with hydrogen peroxide as a fuel.

3 M SPC (sodium percarbonate), contains 4.5 moles of hydrogen peroxide per SPC adduct molecule. 3 M SPC (sodium percarbonate) contains H_2O_2 equal to 3 x 1.5 = 4.5 moles. Therefore, for this study, 4.5 M H_2O_2 was chosen as fuel along with lower concentrations of H_2O_2 as well. The electrolyte for this experiment was 2 M H_2SO_4, which was mixed with an equal volume of the fuel solution. The acidic gel electrolyt was applied between the two paper strips. The polarization curves and OCV for different H_2O_2 concentration as fuel with 0.5 M $KMnO_4$ oxidant (fixed) concentration for all experiments were plotted (fig 7.1.1 e-g).

(44)
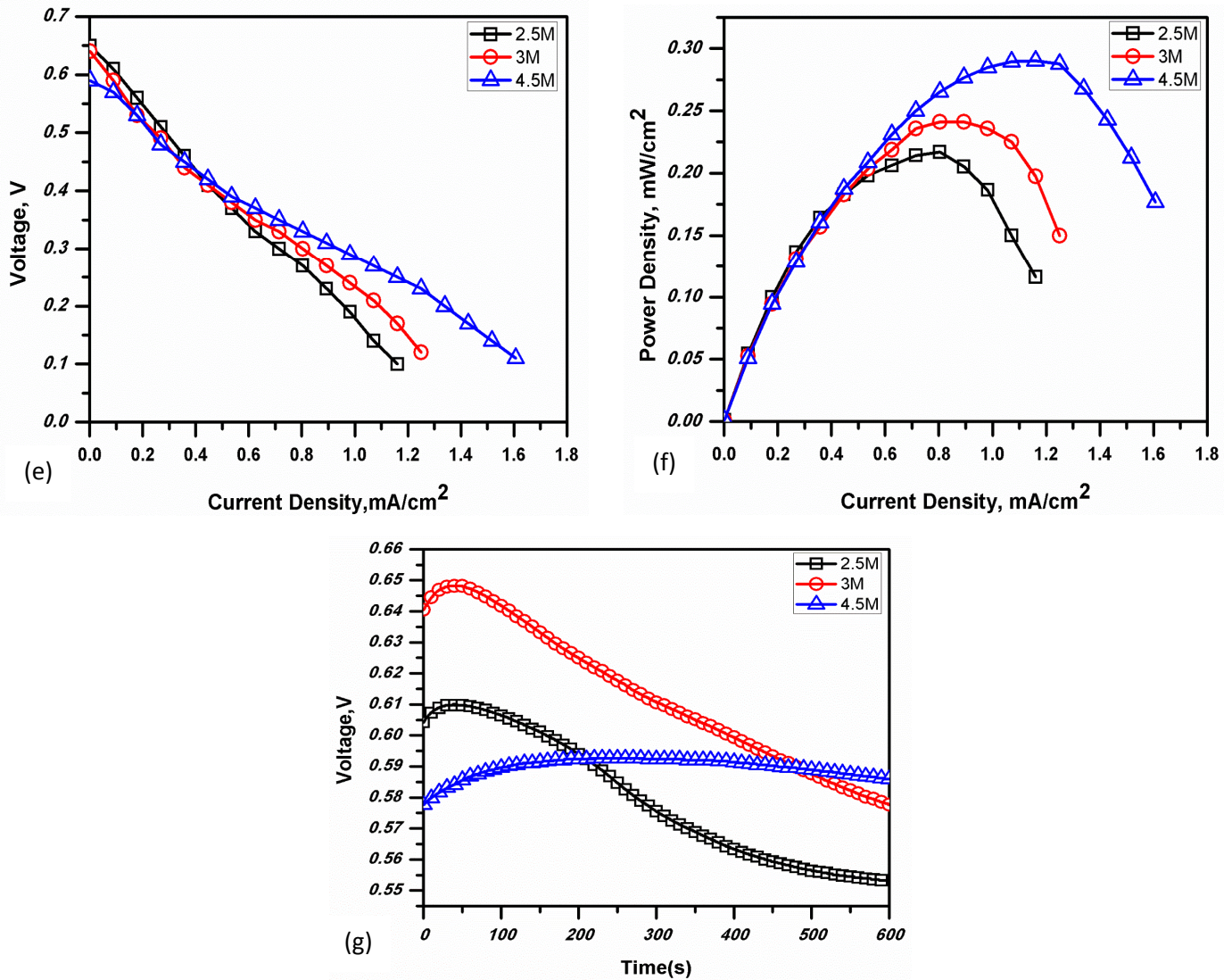
Fig 7.1.1 (e) Voltage vs current density curves and (f) Power density vs current density curves using H_2O_2 as a fuel. (g) OCV vs time curves for H_2O_2 at different concentration comparable to sodium percarbonate.

Here in fig 7.1.1 (e), the voltage drop for different H_2O_2 concentrations was observed with increase in current density. For all concentrations, the voltage is below the theoretical value. From fig 7.1.1 (f), the power density versus current density curves show a maximum power density of 0.3 mW/cm^2 and a maximum current density of 1.6 mA/cm^2. In these curves, the regular trend for increase in current & power densities was seen with increase in the concentration of fuel (H_2O_2), as was observed earlier for the case of sodium percarbonate (SPC) as a fuel.

Voltage versus time curves were plotted for 2.5 M, 3 M and 4.5 M H_2O_2 concentrations [see fig 7.1.1 (g)]. None of the H_2O_2 concentrations is produced OCVs greater than 0.812 V (theoretical

OCV). From this graph, it is clear that H_2O_2 alone as a fuel does not produce a voltage greater than theoretical OCV. But when we used SPC (sodium percarbonate) as a fuel, the OCV is greater than the theoretical value. From these experiments, it was concluded that the increase in experimental OCV is more than the theoretical value due to the contribution made by Na_2CO_3 is present in the sodium percarbonate fuel which might be undergoing a neutralization reaction and is responsible for the increase in voltage when the SPC fuel concentration used is greater than 2.5 M.

7.1.2 Mixed Media

In the following experiment, a basic electrolyte for fuel and an acidic electrolyte for oxidant was used. To make the fuel/oxidant solutions, equal volumes of the fuel / oxidant were mixed with the same amount of basic / acidic electrolytes respectively. They were then dropped on the paper strips to run the cell.

Fuel: $Na_2CO_3.1.5H_2O_2$ (variable concentration from 0.5 M to 3 M)

Electrolyte: NaOH

Fuel: Electrolyte ratio used was 1:1 molar. For 0.5 M fuel concentration, 0.5 M sodium percabonate solution was mixed with an equal volume of 0.5 M NaOH (basic electrolyte). For 2 M fuel concentration, 2 M SPC (sodium percarbonate) and 2 M NaOH solutions were mixed in equal volume.

Oxidant: $KMnO_4$ (concentration fixed at 0.5 M)

A $KMnO_4$ (0.5 M) solution was mixed in equal amount of *H_2SO_4 as an electrolyte* with a fixed concentration of 2 M in all mixed media experiments.

Gel electrolyte: An acidic gel electrolyte was used.

Reactions involved:

A solution of sodium percabonate in water gives the following reaction:

$$2Na_2CO_3.3H_2O_2 \text{ (aq.)} \rightarrow 4Na^+ + 2CO_3^{2-} + 3H_2O_2$$

When a basic electrolyte is mixed with the SPC (sodium percarbonate) fuel then,

$$2Na_2CO_3.3H_2O_2 + NaOH \rightarrow 4Na^+ + 2CO_3^{2-} + 3H_2O_2 + NaOH$$
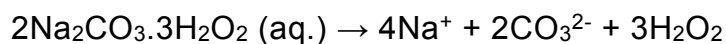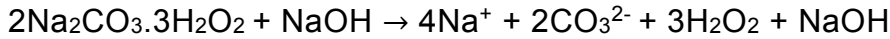
At anode, H_2O_2 (l) + $2OH^-$ → O_2 + $2H_2O$ (l) + $2e^-$

When an acidic electrolyte H_2SO_4 (2M) is mixed with $KMnO_4$ (0.5 M):

At cathode, MnO_4^- + $8H^+$ + $5e^-$ → Mn^{2+} + $4H_2O$ (l)

The redox chemical reaction are [19]:

MnO_4^- + $8H^+$ + $5e^-$ → Mn^{2+} + $4H_2O$ (l)	$E^\circ{}_{red.}$= 1.506 V
H_2O_2 (l) + $2OH^-$ → O_2 + $2H_2O$ (l) + $2e^-$	$E^\circ{}_{ox.}$= 0.0649 V
$2MnO_4^-$ + $6H^+$ + $5H_2O_2$ (l) → $2Mn^{2+}$ + $8H_2O$ (l) + $5O_2$	$E^\circ{}_{cell}$= 1.57 V
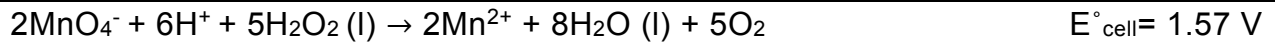
The polarization curves for T-shaped paper based cell for mixed media are given below (*fig 7.1.2).*
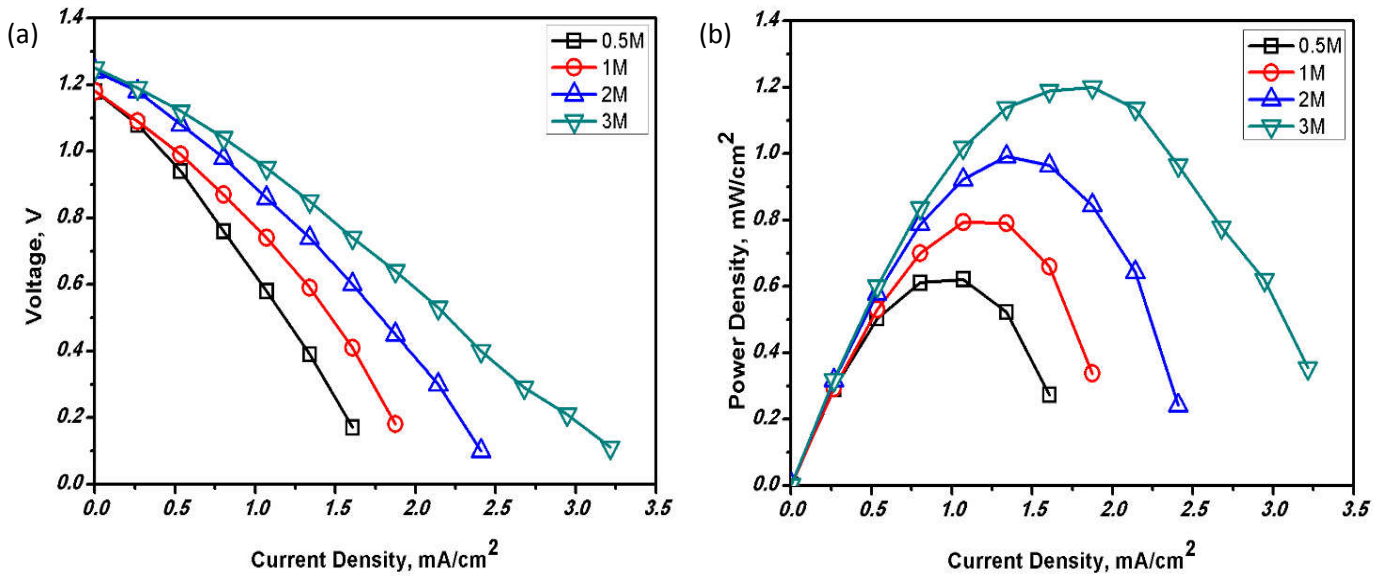
Fig 7.1.2 (a) Current density vs voltage curves at different fuel concentrations with same oxidant concentration. (b) Power density vs current density plots for different fuel concentrations with same oxidant concentration.

From the result of the T-shaped mixed media experiments, the maximum current density and power density obtained are 3.214 mA/cm² and 1.2 mW/cm² respectively at the optimum

(47)

fuel concentration of 3 M. From 7.2.1 (a), it is observed that increasing the concentration of fuel, the current density increases for more number of hydrogen peroxide molecules are available and these get oxidized to give electrons at the anode. As the number of electrons increases at the anode, the current density increases. The power density polarization curves also show a regular trend in the increase of maximum power density with increasing fuel concentration 0.5 M to 3 M. This is due to the OCV increases linearly with fuel concentration [see fig 6.4 (b)]. At the anode, more fuel molecules release more electrons; these two factors contribute towards a linear increase in maximum power density with respect to respective fuel concentration [see fig 7.2.1 (b)].

XRF- (X-ray fluorescence spectroscopy) studies on the fuel and oxidant strips were separately performed to determine the elements (in the form of ions) that migrate/shuttle between the two- L shaped anodic and cathodic strips through the acidic gel electrolyte.

fuel strip 1

Compound	Mg	Al	Si	P	S	Cl	Ca	Mn	Fe	Cu	As	Eu	Pb
Conc	7.217	3.559	4.411	6.005	39.648	18.004	13.369	6.734	0.924	0.083	0.006	0.000	0.041
Unit	%	%	%	%	%	%	%	%	%	%	%	%	%

fuel strip 2

Compound	Mg	Al	Si	P	S	Cl	Ca	Mn	Fe	Eu
Conc	0.000	0.000	3.980	5.585	58.580	17.497	12.951	0.825	0.584	0.000
Unit	%	%	%	%	%	%	%	%	%	%

sample paper (whatmann filter paper)

Compound	Mg	Si	P	Cl	Ca	Fe
Conc	21.462	10.350	15.049	24.225	27.930	0.984
Unit	%	%	%	%	%	%

Al- coming due to strips were kept in the Al-foil.

The XRF data- sample paper is a blank Whatman filter paper and the fuel strips: 1 and 2 are taken for reproducibility of results for the same mixed media experiment with optimum 3 M concentration of fuel and fixed oxidant (0.5 M $KMnO_4$) concentration. Only sodium percarbonate ($Na_2CO_3.1.5H_2O_2$) and NaOH are present at the anodic side strip but the XRF data for the fuel strip shows Sulphur in good amount along with a small amount of Manganese. Other elements originate from the Whatmans filter paper strip. Mn^{2+} ions cannot migrate from the cathode to anode for the negative cathode electrode gains electrons.

Therefore, due to a high amount of Sulfur detected on the fuel strip, it is concluded that migration of SO_4^{2-} ions occurs from the cathode to the anode through the gel electrolyte. This is probably responsible for the high current in the mixed media case.

(48)

oxidant 1

Compound	Al	Si	P	S	Cl	K	Ca	Sc	Ti	Mn	Pr
Conc	2.242	0.890	1.095	25.877	2.557	16.626	1.922	0.000	0.020	48.729	0.044
Unit	%	%	%	%	%	%	%	%	%	%	%

OXIDANT 2

Compound	Mg	Al	Si	P	S	Cl	K	Ti	Mn	Ni	Cu	Rb	Yb
Conc	0.332	1.440	1.096	0.621	22.368	0.948	17.586	0.027	55.534	0.019	0.006	0.004	0.020
Unit	%	%	%	%	%	%	%	%	%	%	%	%	%

sample paper (whatmann filter paper)

Compound	Mg	Si	P	Cl	Ca	Fe
Conc	21.462	10.350	15.049	24.225	27.930	0.984
Unit	%	%	%	%	%	%

Al- coming due to strips were kept in the Al-foil.

$KMnO_4$ and H_2SO_4 are present on the oxidant strip. No ion migrated from the anode side to cathode side. Al is present because the strips were wet with solutions and were kept in Al-foil for XRF. Sodium ions were not detected due to shortage of helium gas that was required by the instrument to detect Na.

Therefore, a good current was achieved by the cell due to the migration of SO_4^{2-} ions from the cathode to the anode side and the sodium ions present at the anode side react to form Na_2SO_4 salt.

7.1.3 Basic Media

In the experiment on T-shaped paper based cells, only a basic electrolyte is used for both the fuel and oxidant. An alkaline gel electrolyte was used between the two paper strips.

To prepare the fuel, equal volumes of SPC (sodium percarbonate) solution is mixed with an equal volume of the basic electrolyte. Similarly, equal volumes of the $KMnO_4$ solution and the basic electrolyte are mixed for the oxidant solution. To run the cell, the fuel solution and the oxidant solution were dropped on the paper strips.

Fuel: $Na_2CO_3.1.5H_2O_2$ (variable concentration from 0.5 M to 3 M)

Oxidant: $KMnO_4$ (concentration fixed, 0.5 M)

Electrolyte: NaOH (3 M, fixed for both fuel and oxidant)

Gel electrolyte: alkaline gel electrolyte was used.

The Reactions involved are given below.

A solution of sodium percabonate in water gives the following reaction.

$$2Na_2CO_3.3H_2O_2 \text{ (aq.)} \rightarrow 4Na^+ + 2CO_3^{2-} + 3H_2O_2$$

(49)
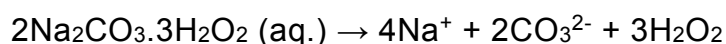
When a basic electrolyte is mixed with the SPC (sodium percarbonate) fuel ($2Na_2CO_3.3H_2O_2$ + NaOH) and a fuel solution is dropped on the anodic side of the cell.

At the anode, H_2O_2 (l) + $2OH^-$ → O_2 + $2H_2O$ (l) + $2e^-$
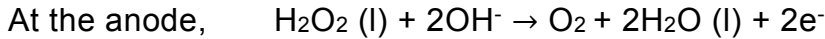
When a basic electrolyte NaOH (3 M) is mixed with $KMnO_4$ (0.5 M):

At cathode, MnO_4^- + $2H_2O$ + $3e^-$ → MnO_2 + $4OH^-$
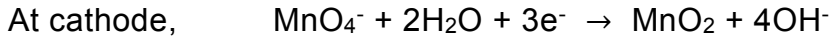
The redox chemical reactions are given below [19].

MnO_4^- + $2H_2O$ + $3e^-$ → MnO_2 + $4OH^-$ E°_{red}= 0.588 V

H_2O_2 (l) + $2OH^-$ → O_2 + $2H_2O$ (l) + $2e^-$ E°_{ox}= 0.0649 V

---

2 MnO_4^- + 3 H_2O_2 → 2 MnO_2 + $3O_2$ (g) + $2OH^-$ + $2H_2O$ E°_{cell}= 0.6529 V
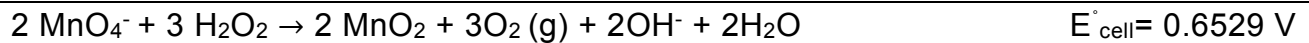
The polarization curves for the T-shaped paper based cell for all basic media (*fig 7.1.3*) are given below.

(a)   (b)
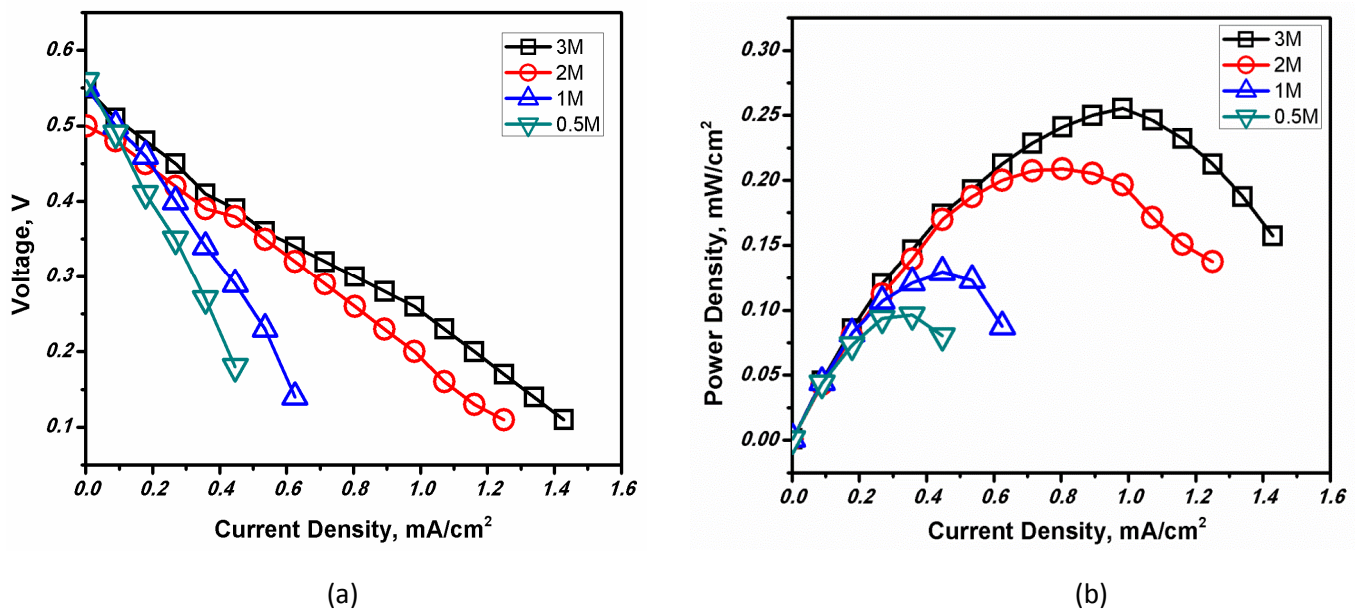
Fig 7.1.3 (a) Current density vs voltage curve at different fuel concentrations by keeping the oxidant concentration same for all basic media cell experiments. (b) Power density vs current density plots for different fuel concentrations with same oxidant concentration for all basic media cell experiments.

From the results of polarization curves for all basic media experiment, the cell shows a maximum current density = 1.43 mA/cm² and a maximum power density = 0.255mW/cm² at 3 M fuel concentration. The optimum concentration of fuel is 3 M. 0.48V is the OCV of this

cell at optimum 3 M concentration. From the plot [fig 7.1.3 (a)], the curve shows a decrease in voltage with increasing current density as the SPC fuel concentration increases from 0.5 M to 3 M. This is due to an increase in fuel availability at the anode, more hydrogen peroxide molecules undergo oxidation and this results in an increase in current hence the current density increases. Similarly, increase in OCV with increase in fuel concentration is due to more species are available for oxidation at the anode. Power density also increased from 0.5 M to 3 M fuel [fig 7.1.3 (b)] concentration.

----------------=====-----------------=====-----------------=====----------------

Since, the mixed media experiment on a T-shaped cell gave highest current density and power density at an optimum 3 M sodium percarbonate fuel concentration, other detailed studies were performed on the T-shaped cell by using only the mixed media configuration.

----------------=====-----------------=====-----------------=====----------------

7.2: Gel electrolyte characterization

In this section, a study of gel electrolyte is provided by using a T-shaped mixed media paper based fuel cell.

7.2.1 Study of T-shaped mixed media cell with or without an acidic gel electrolyte

Mixed Media assembly	With acidic gel	Without gel
Fuel: SPC (sodium percarbonate, 3 M) with NaOH (3 M) basic electrolyte.	OCV = 1.22 V	OCV = 1.22 V (same)
Oxidant: KMnO$_4$ (0.5 M) with acidic electrolyte H2SO4 (2 M).	Max. current = 3.08 mA	Max. current = 0.02 mA

From this experiment, it was concluded that without an acidic gel electrolyte, ion transport does not occurs to produce current. Therefore a gel electrolyte is one necessary for an efficient working of a T-shaped paper based fuel cell.

7.2.2 Study of T-shaped mixed media cell with acidic and alkaline gel membrane

Mixed Media assembly	With acidic gel	With alkaline gel
Fuel: SPC (sodium percarbonate, 3 M) with NaOH (3 M) as a basic electrolyte.	OCV = 1.22 V	OCV = 1.21 V (same)
Oxidant: KMnO$_4$ (0.5 M) with an acidic electrolyte H$_2$SO$_4$ (2 M).	Maximum current = 3.08 mA	Maximum current = 1.56 mA

Since the experiment on the T-shaped mixed media with an acidic gel produced more current than with the alkaline gel, we proceeded with further studies by only using an acidic gel membrane in the T-shaped mixed media paper based fuel cells.

7.2.3 Performance of a 3 M SPC T-shaped mixed media cell with different concentrations of acidic gels
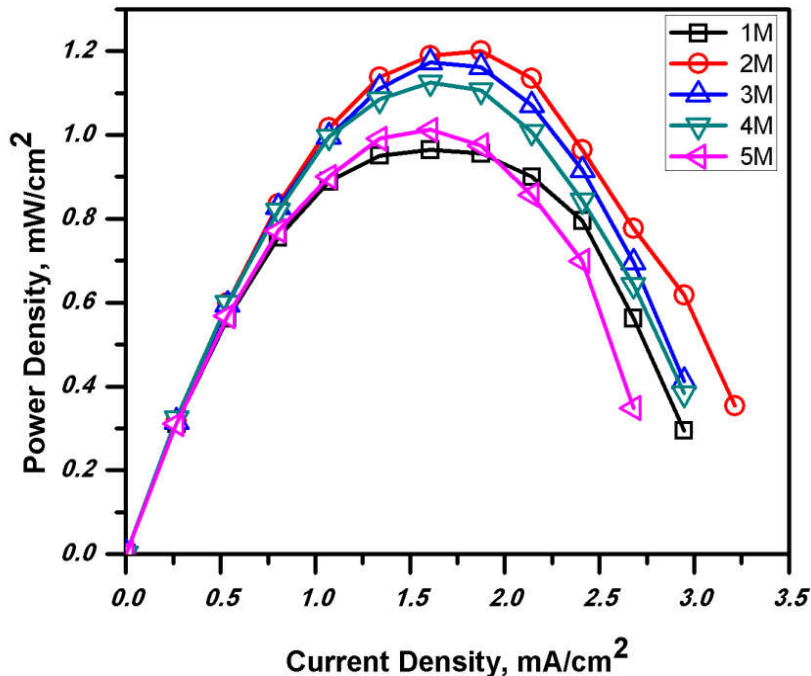

Fig 7.2.3 Study of acidic gels with different concentrations on T-shaped mixed media cells using a 3 M fuel concentration and a 0.5 M oxidant concentration.

In this study of acidic gels, the experiments were done with different acidic gel compositions with varying H_2SO_4 electrolyte concentrations of 1 M, 2 M, 3 M, 4 M & 5 M. The performances were evaluated by LSV at 3 M SPC fixed fuel concentration and 0.5 M $KMnO_4$ fixed oxidant concentration for mixed media cells. From the polarization curves (fig 7.2.3), the cell producing maximum power at 2 M concentration for the acidic gel. The maximum power density peak increases initially with gel concentration (1 M to 2 M) and then decreases 3 M to 5 M. conc. 3 M. The cell produces a maximum power density = 1.2mW/cm^2 at 2 M optimum concentration of the acidic gel. This is due to when concentration increased from an increase in the electrolyte concentration of the gel from 1 M to 2 M. The increase in electrolyte concentration is responsible for the facile ion transport but the power density decreases slightly after 2 M. At low concentration of the acidic gel (1 M to 2 M), the ions are dissociated but at high concentrations of the gel, the ion-pairs form which cause the decrease in the conductivity of gel. Hence, at a concentration of the gel > 2M, the power density decreases as the concentration of gel increases. *Thus the optimum acidic gel concentration was fixed at 2 M for further studies.*

7.2.4 Effect of temperature on the conductivity of a 2 M-acidic gel

The effect of temperature was studied over temperature range from 10°C to 90°C on the acidic gel with an optimum 2 M concentration. The conductivity of 2M acidic gel membrane is almost the same over the entire range of temperature. The conductivity is of the order of x 10^{-3} S/cm in this range.

At low temperature, the viscosity of the gel increases and as a result a minor decrease in conductivity is observed. At the higher temperatures, the viscosity decreases, ion-mobility increases, so conductivity increases.
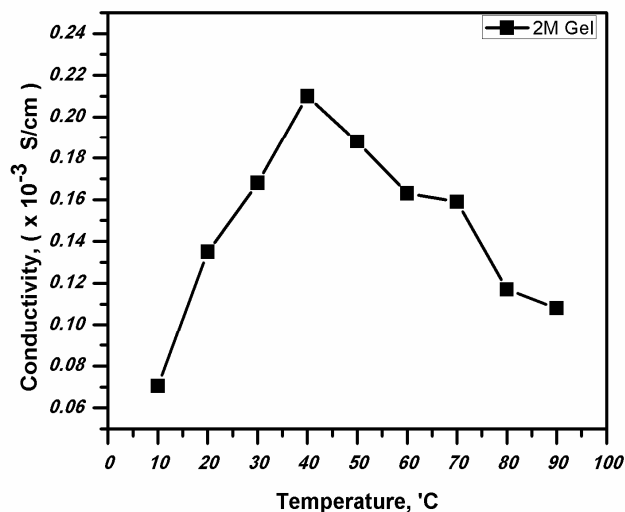

Fig 7.2.4 Conductivity variation of the acidic gel (2 M) at different temperatures.

7.3 T-shaped mixed media cell with gold nanoparticles (NPs) as catalysts

Preparation of gold NPs [22]:

A 0.5 wt% aqueous solution of $HAuCl_4$ was prepared and stored in a fridge at 4˚C before use. 1 mL of $HAuCl_4$ solution and 42.5 µL of $AgNO_3$ (0.1 wt %) solutions were mixed in a 10 mL beaker. Then, 1 mL of an aqueous citrate solution (1 wt %) was poured into the beaker and deionised-water was added such that the total volume was which is a solution of gold NPs 2.5 mL. The solution was kept in a fridge at 4˚C for 5 mins. 47.5 mL of water were placed in a two necked round bottom flask with a condenser and kept for heating to boil. After 10 mins of heating, 2.5 mL of a cold mixture of $HAuCl_4$/$AgNO_3$/citrate was injected in to the hot boiling water under vigorous stirring. The color of the solution changed from yellow to grey. Refluxing was continued for the mixture for 1 h.

A Clear pink color solution was obtained [22], which is a solution of gold NPs.

Characterization of NPs

NPs were characterized by using UV-visible spectroscopy and scanning electron microscopy (SEM).
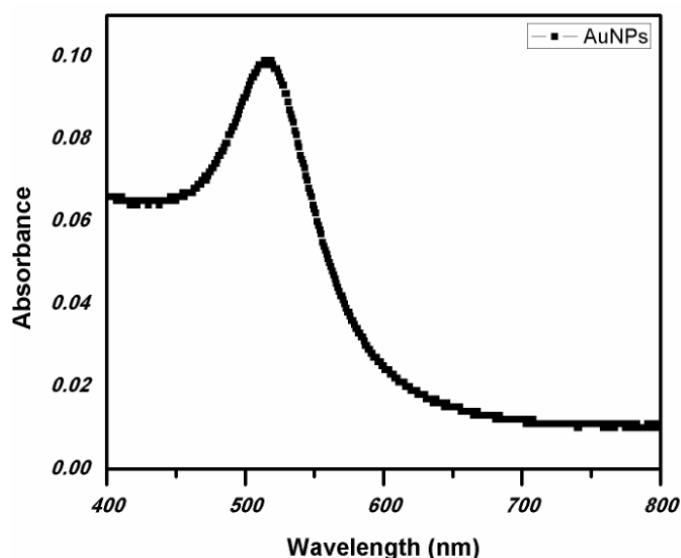
Fig 7.3 (a) A UV-Visible spectroscopy of gold NPs.

Fig 7.3 (b) A photograph of a gold NPs colloid.

The UV-Visible spectrum of gold NPs shows a surface plasmon resonance peak at 519 nm. The size of the NPs is expected to be in the range of 12 to 25 nm [22]. The gold NPs solution was kept in fridge.
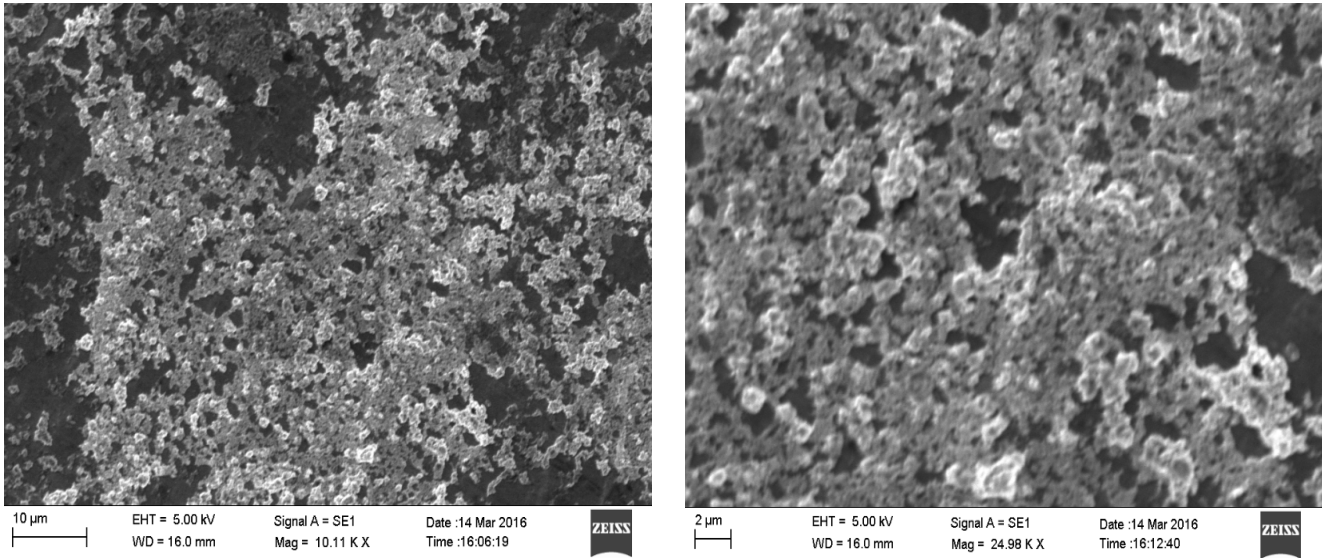
Fig 7.3 (c) SEM-images of gold NPs.

The SEM images of Au-NPs [fig 7.3 (c)], shows aggregated NPs, which are interconnected.

Polarization curves with gold NPs as catalysts on T-shaped mixed media cell

1) To evaluate catalytic performance of gold NPs at electrode/electrodes, experiments were done with a 3 M SPC optimum fuel concentration and 0.5 M KMnO₄ oxidant concentration. *(The Au-NPs solution was dropped on graphite electrodes and dried by blowing air).*
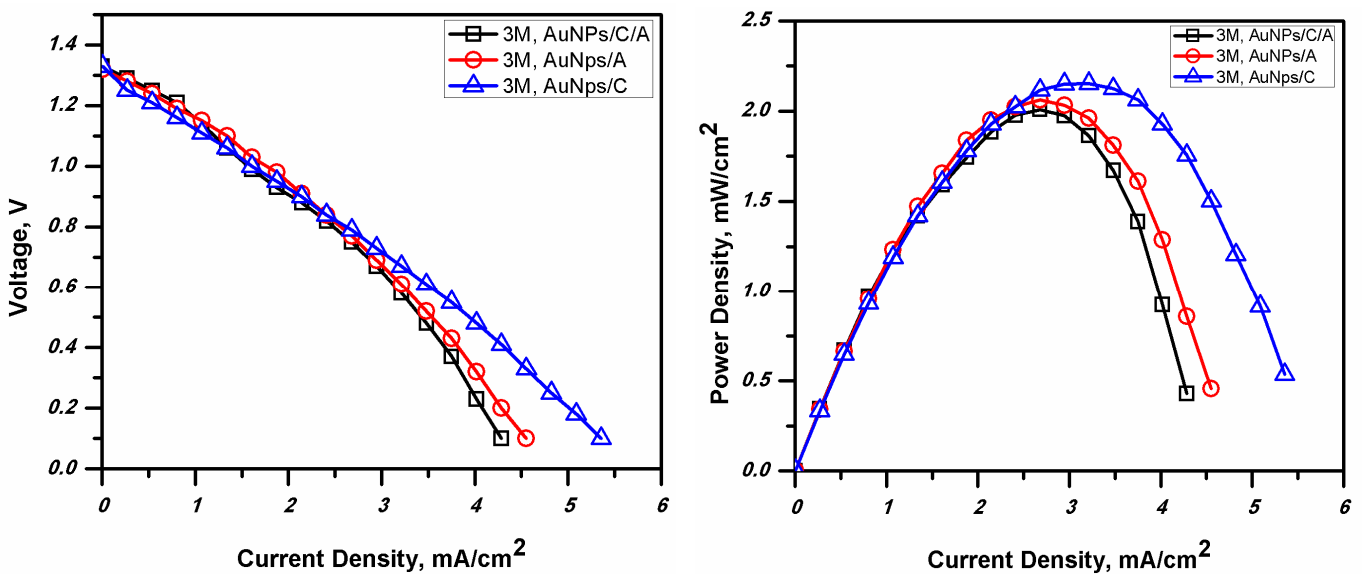
Fig 7.3 (d) Polarization curves for T-shaped mixed media cells with Au NPs at 3 M SPC fuel concentration. Voltage vs current density curves and power density vs current density are curves.

(55)

The Au NPs were drop casted on the cathode and/or anode (graphite). Drop-casting was done three times, and after each time, the electrode was dried. From the polarization curves of voltage vs current density and power density vs current density shown in fig 7.3 (d), it is observed that the Au NPs showed the best performance when deposited only at the cathode. A maximum current density = 5.357 mA/cm^2 and maximum power density = 2.15 mW/cm^2 was obtained. The performance decreases slightly when deposited only at the anode and an almost similar result was obtained when Au NPs were deposited at both anode and cathode. Au NPs catalyze the cathodic reaction effectively in comparison to the anodic reaction. So, we studied the effect of fuel concentration with Au NPs deposited only at cathode.

2) Au NPs as catalysts on cathode in T-shaped mixed media cells with different fuel concentrations and 0.5 M KMnO$_4$ as oxidant
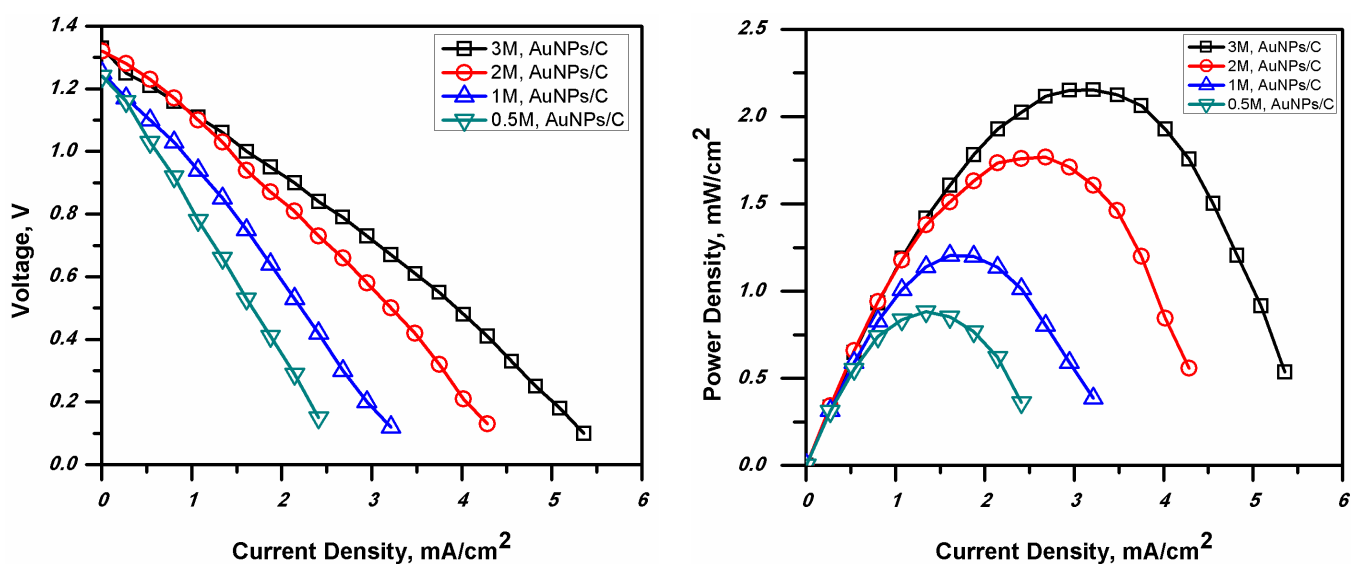
Fig 7.3 (e) Polarization curves for T-shaped mixed media cells with Au NPs (at cathode) with varying fuel concentration (0.5 M to 3 M SPC) and constant oxidant concentration (0.5 M KMnO$_4$). Voltage vs current density curves and power density vs current density curves are plotted.

In all experiments, with different fuel concentrations, Au NPs was deposited only at the cathode. The maximum current density and maximum power density obtained are 5.357 mA/cm^2 and 2.15 mW/cm^2 respectively. There is an increase in performance for each fuel concentration with catalyst compared to the performance at same fuel concentration [*see fig 7.1.2*] without AuNPs as catalyst.

(56)

7.4 Au/NiO composite as catalysts in T-shaped mixed media cells

Preparation of an Au/NiO composite [24]:

To prepare Au/NiO with 4% Au content, a 5 mmol solution of $HAuCl_4$ and $Ni(NO_3).6H_2O$ was prepared, using 0.2 mmol $HAuCl_4$ and 4.8 mmol $Ni(NO_3).6H_2O$. These were dissolved completely in a combination of mixed solvents of 15 mL deionized water and 60 mL of ethanol under agitation. Then, 0.3 g of dioctyl sulfosuccinate sodium salt (surfactant) and 20 mmol of urea were added to the above mixture and kept for stirring for 20 mins. Finally, the mixture was poured into a Teflon-lined stainless steel autoclave, sealed and placed in an oven for 12 h at 120˚C.

The prepared precursor was centrifuged and washed first with deionized-water, and then with absolute alcohol (ethanol) three times. The precursor was dried in a vacuum oven for 10 h maintained at 80˚C.

Lastly, the dried precursor was calcinated at 350 ˚C for 3 h.
The Au/NiO product prepared with 4% Au content was black in color.

Calcination at 350˚C
For 3hours

Dried precursor
(Before calcination)

Au/NiO composite
(After calcination)
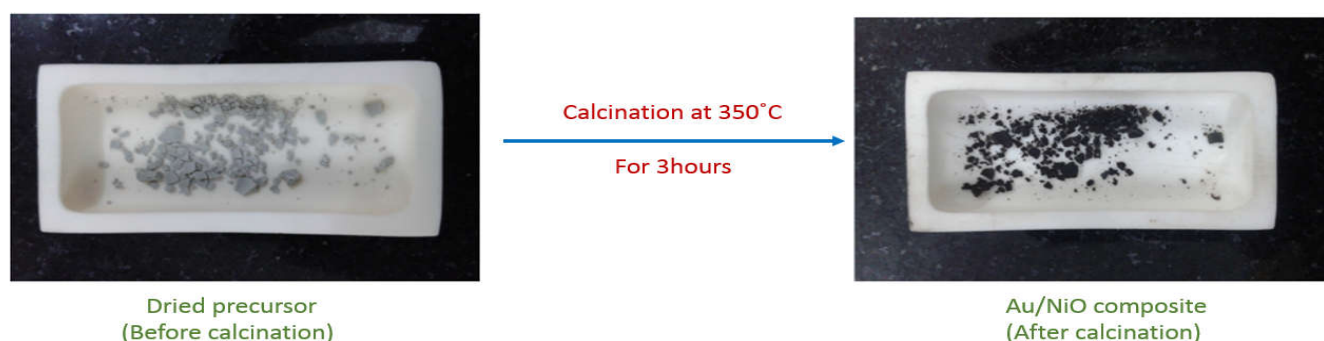
Fig 7.4 (a) The formed product (Au/NiO) was black in color after calcination process.

Characterization of Au/NiO composite

This composite is primarily characterized by powder XRD and SEM.
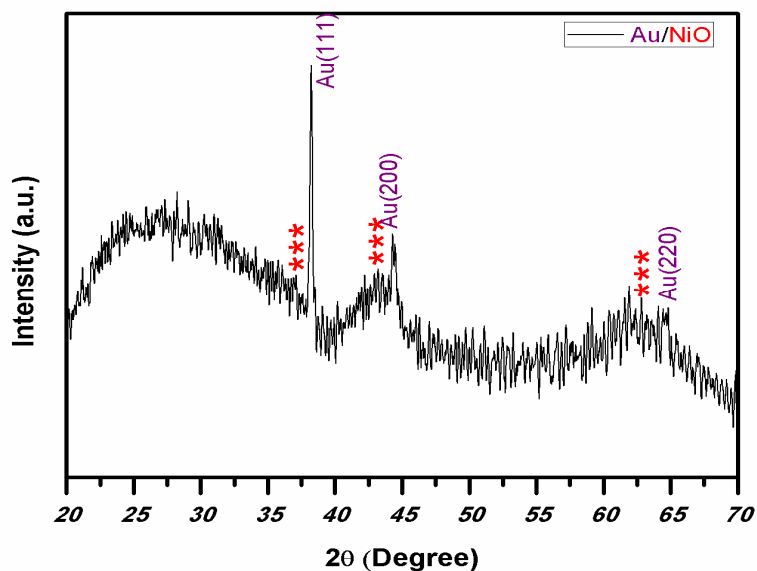
Fig 7.4 (b) XRD pattern of the Au/NiO composite.

Fig 7.4 (c) Photograph of the Au/NiO Composite.

The XRD peaks of Au in the Au/NiO composite match with the diffraction peaks of Au with a face centered cubic lattice. The positions where NiO peaks are expected, are marked with asterisks [see fig 7.4 (b)].

SEM Images of Au/NiO:
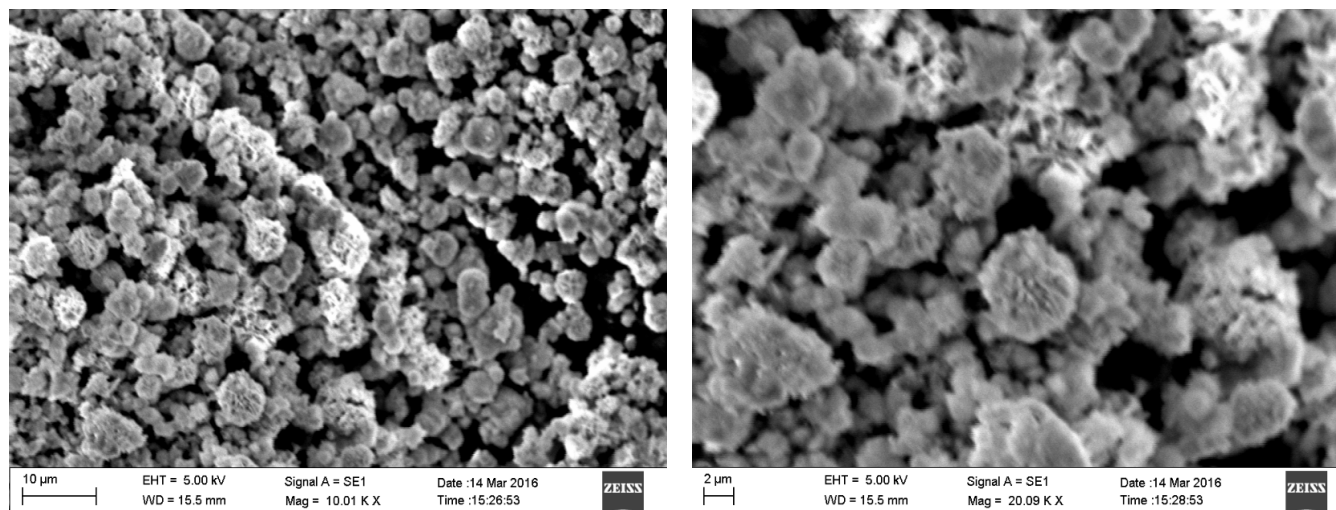
Fig 7.4 (d) SEM images of Au/NiO composite.

The morphology of the Au-NiO composite reveals the presence of inter-linked porous particles, indicating that the effective surface area available for the redox reactions is reasonably high.

(58)

<u>Polarization curves with Au/NiO composite as catalyst on T-shaped mixed media cells:</u> *(Au/NiO composite was dissolved in ethanol and this solution drop-casted on the graphite electrodes and air-blow dried).*

Fig 7.4 (e) Polarization curves of Au/NiO composite on T-shaped mixed media cells with Au/NiO composite as catalysts, with 3 M SPC fuel concentration and same oxidant concentration (0.5 M KMnO$_4$), Voltage vs current density curves and power density vs current density curves are plotted.

The T-shaped mixed media cell with 3 M SPC fuel generates a maximum current density = 5.625mA/cm^2 and maximum power density = 2.6625 mW/cm^2. These values were obtained when the Au/NiO catalyst was deposited on both anode and cathode.

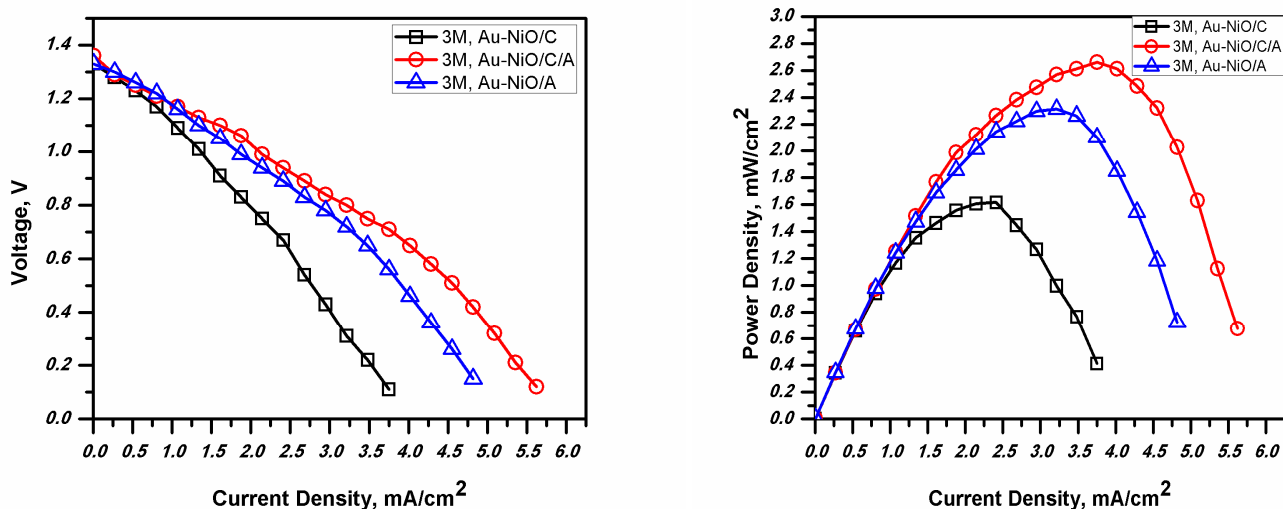When the catalyst Au/NiO was deposited on both the graphite electrodes, the cell performance is maximized. This is because the Au/NiO composite is porous in nature, which catalyzes both the anodic as well as cathodic reactions. The performance observed for the cell with the Au/NiO composite on both electrodes is superior to the performances of the cells with the Au/NiO catalyst on any one of the two electrodes.

Since, at the anode, the anoyte is sodium percarbonate in a basic electrolyte (NaOH), NiO is more stable in a basic solution as compared to an acidic solution. This may be the reason for increased power density and current density performance for Au/NiO composite only at anode, compared to the performance of the cell with Au/NiO only at cathode. At the cathode electrolyte is sulfuric acid, and in catholyte stream, NiO slowly forms Ni(OH)$_2$ upon reacting with the acid which causes performance decline [25].

Electrochemical Impedance studies (EIS)

7.5 Impedance studies of T-shaped mixed media SPC fuel cells

The impedance plots for the T-shaped mixed media paper based fuel cells were obtained by EIS (electrochemical impedance spectroscopy) measurements. We have done EIS for 0.5 M, 1 M, 2 M and 3 M SPC fuel concentration were used. In these experiments, the oxidant [KMnO$_4$ (0.5 M)] concentration was kept constant.
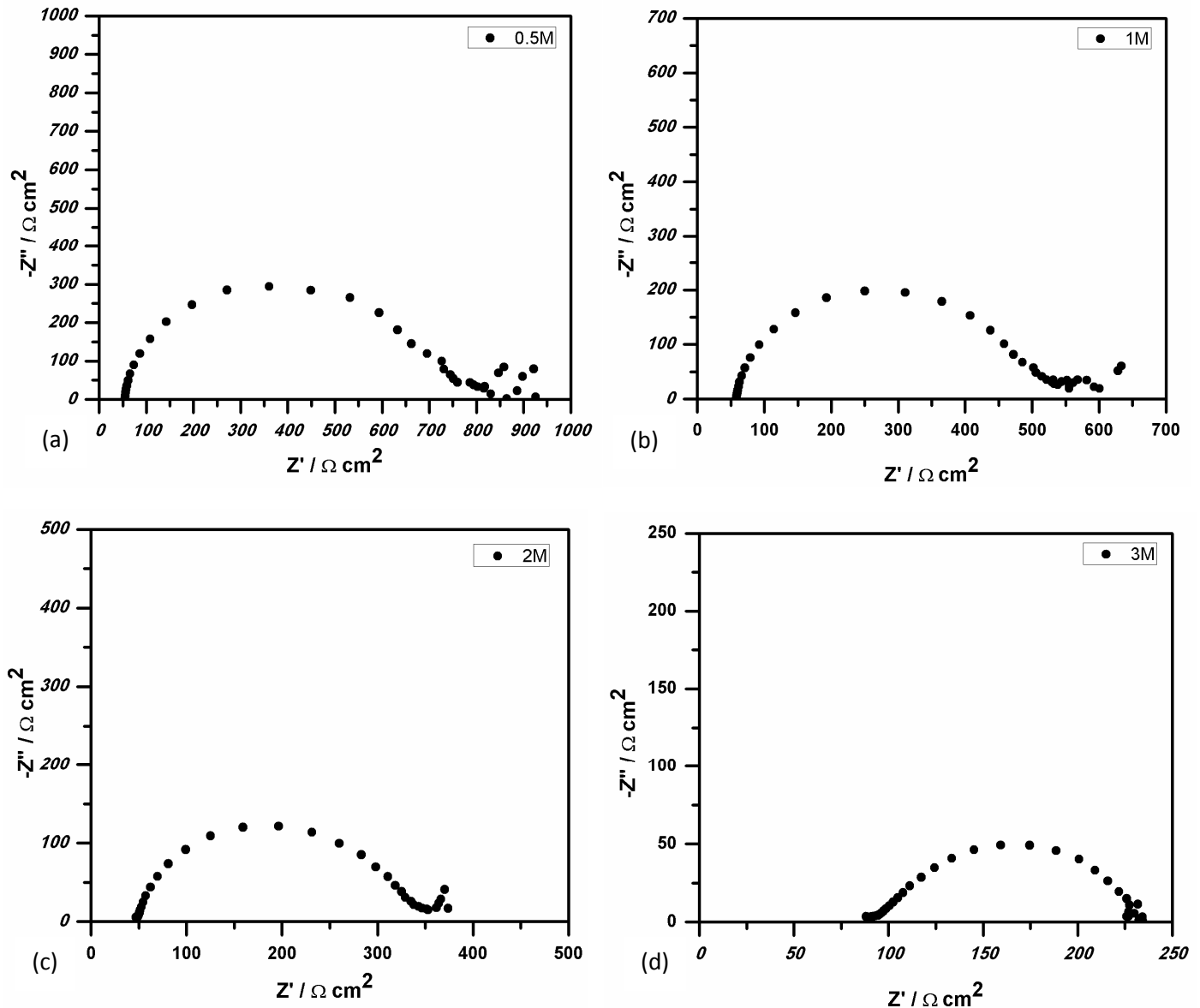
Fig 7.5.1 Nyquist plots for T-shaped mixed media cell with different concentration of SPC fuel and fixed 0.5M KMnO$_4$ as oxidant. (a)0.5M SPC, (b)1M SPC, (c)2M SPC, (d)3M SPC concentration represented on lower left of the curves.

EIS plots for the T-shaped mixed media cells, were obtained by applying 10 mV sinusoidal perturbation in the set frequency range of 1 MHz to 0.1 Hz at OCV. The Nyquist curves provides information about the resistances of the operating cell. Fig 8.1.1 (a) for 0.5 M (b) for 1 M (c) for 2 M SPC fuel concentration, cells show a narrow frequency region over which the mass transfer effect was observed. The resistances of the cells at different concentration of fuels, by the interpretation of each Nyquist plot are given below.

Resistance Ω cm^2	0.5 M SPC	1 M SPC	2 M SPC	3 M SPC
Ohmic resistance R_Ω	56.3 Ω cm^2	57.8 Ω cm^2	50.6 Ω cm^2	88.1 Ω cm^2
Polarization Resistance (R_p)	802.3 Ω cm^2	497.6 Ω cm^2	302.17 Ω cm^2	145.8 Ω cm^2
Total resistance	858.6 Ω cm^2	555.4 Ω cm^2	352.8 Ω cm^2	234.45 Ω cm^2

When the fuel concentration was increased from 0.5 M to 2 M, **R_Ω (Ohmic resistance)** remains almost the same and with further increase in fuel concentration, increase in Ohmic resistance was observed i.e., 3 M. This may be due to CO_2 molecules accumulated at the anode (graphite electrode). At higher concentration, 3 M, the sodium percarbonate fuel releases more Na_2CO_3 along with H_2O_2 in the solution of anolyte and Na_2CO_3 gives the following reaction.

$$CO_3^{2-} + H_2O \rightarrow HCO_3^- + OH^-$$

$$HCO_3^- + H_2O \rightarrow CO_2\,(g) + OH^-$$
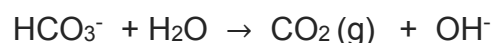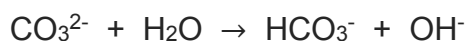
So, at a lower concentration, CO_2 evolution and accumulation is lower and thus does not affect the Ohmic resistance but at a higher concentration (3 M), more CO_2 is evolved. Hence increase in Ohmic resistance for 3 M SPC fuel concentration, was observed.

A systematic decrease in **R_p (polarization resistance)** was observed from 0.5 M to 3 M SPC fuel concentration. These resistances decrease with increase in fuel availability. At high concentration, more number of hydrogen peroxide molecules oxidize and produce more electrons which lowers R_p.

Therefore, the combination of the R_Ω and R_p, yields total resistance, which decreases with increasing concentration of fuel. We have also plotted the Bode phase & Bode modulus versus frequency for different concentrations of fuel in T-shaped mixed media cell experiment, to know the nature of the operating cell.
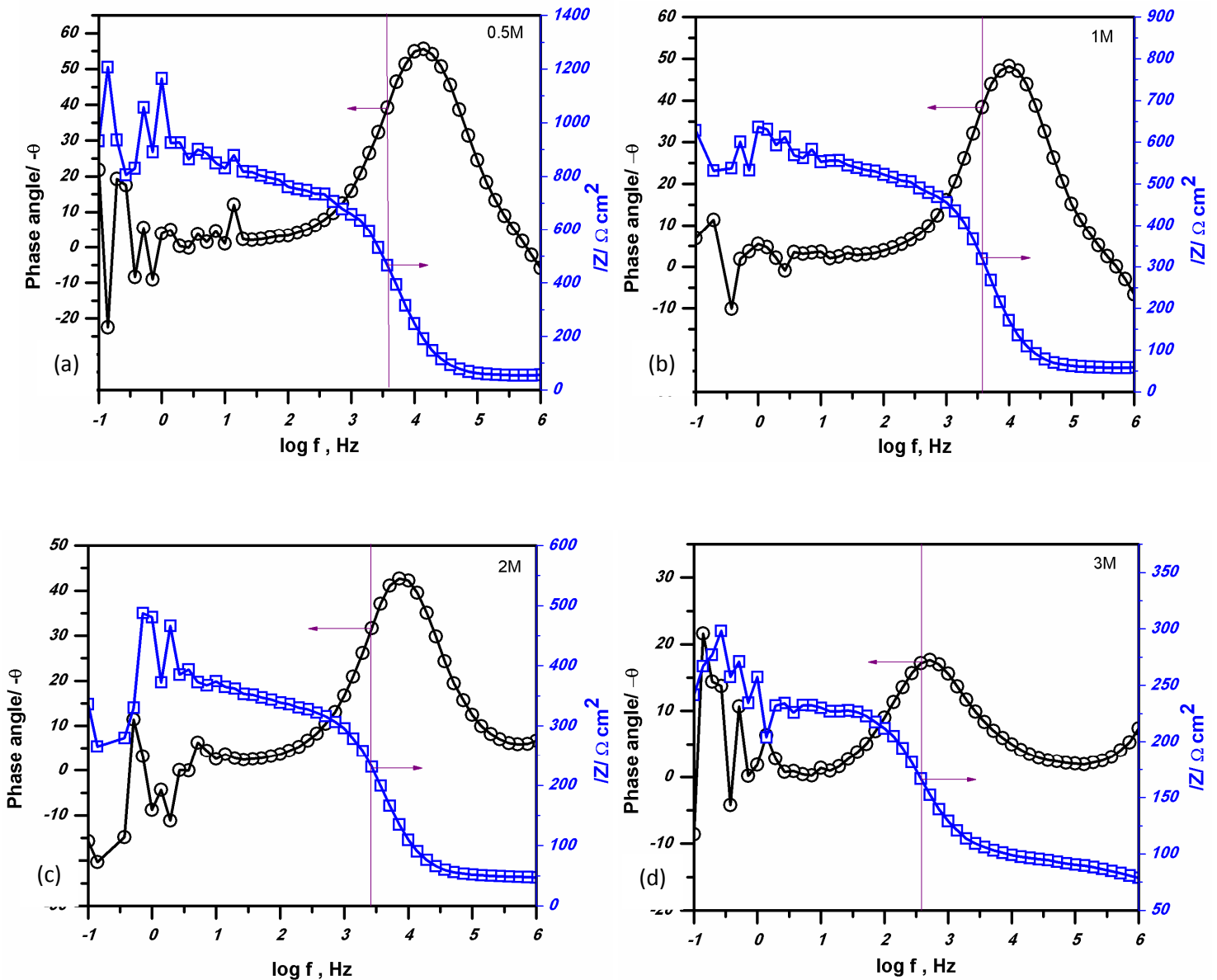

Fig 7.5.2 Bode plots for the T-shaped mixed media cells with different concentrations of SPC fuel and fixed 0.5 M KMnO$_4$ as oxidant. (a) 0.5 M SPC, (b) 1 M SPC, (c) 2 M SPC and (d) 3 M SPC concentrations were used.

From the bode plots, we have collected results for 0.5 M, 1 M, 2 M and 3 M SPC fuel concentration.

Characteristics	0.5 M	1 M	2 M	3 M
Frequency Log f (Hz)	3.571 Hz	3.571 Hz	3.43 Hz	2.571 Hz
Phase (-θ)	39.191 °	38.345 °	31.702 °	17.169 °
Modulus, /Z/	465.19 Ω cm^2	319 Ω cm^2	230.8 Ω cm^2	166.7 Ω cm^2

For all the concentrations of the SPC fuel, the T-shaped mixed media cell at characteristic frequency gives the phase angle in between -17 and -40 degrees, the indicating that this cell does not follow the ideal Randles circuit at any concentration of the SPC fuel and the process cannot be represented by a RC circuit. The phase angle reaches at -45 degree for a pure RC circuit, at characteristic frequency [27].

7.6 Impedance of a T-shaped mixed media cell at V = 0.64 V where maximum power density was obtained using 3 M SPC concentration

We have done the EIS measurements for the T-shaped mixed media cell with 3M SPC fuel concentration at the set potential V = 0.64 V. This voltage corresponds to the maximum power density obtained for 3M SPC fuel cell. This EIS experiment was done to determine the resistances of cell, where the cell yields maximum power.
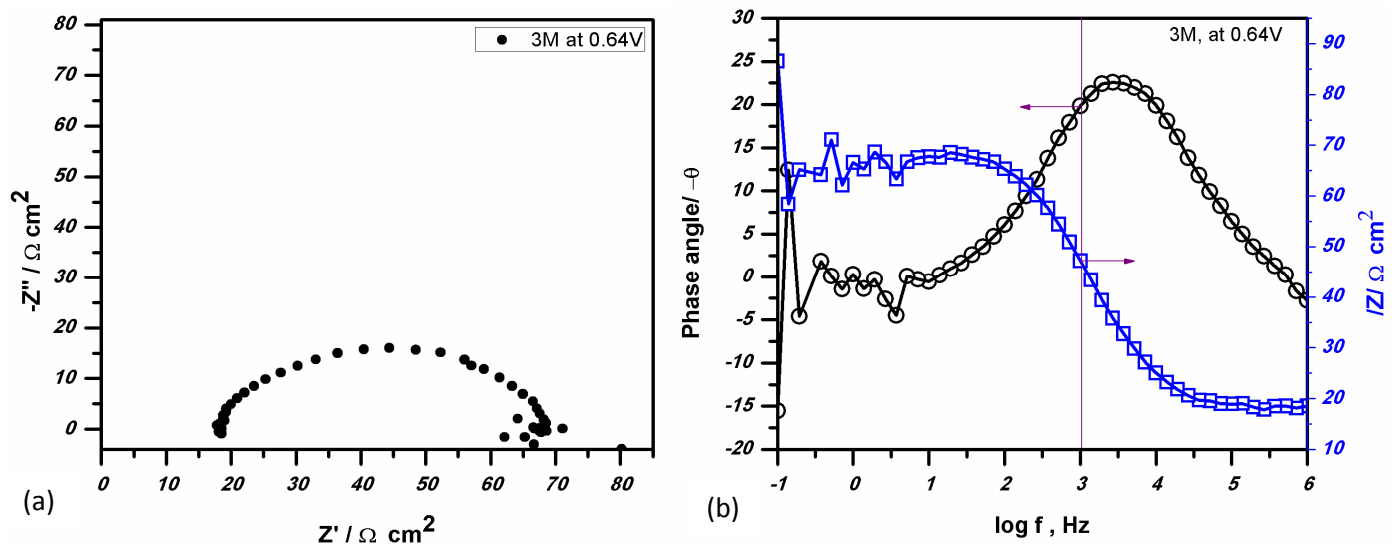
Fig 7.6 (a) Nyquist plot and (b) Bode plot for 3 M SPC concentration at a set potential of 0.64 V, which corresponds to the maximum power density for 3 M SPC fuel in the T-shaped mixed media paper based cell.

From the Nyquist plot (fig S.5), it is observed that for 3 M SPC fuel concentration at 0.64 V, the Ohmic resistance (R_Ω) are decreased to **18.5 Ω cm^2** and polarization resistance (R_p)

decreased to **50 Ω cm²** and therefore **total resistance** decreased to **68.5 Ω cm²**. No mass transport observed. The results are similar to 3 M SPC concentration, at its' OCV. The total resistance of the cell operated with 3 M SPC fuel concentration decreased at 0.64 V as compared to its OCV (1.22 V).

The characteristic frequency = 2.999 Hz, phase angle = -19.8577˚ and /Z/ = 45.19876 Ω cm² for 3 M SPC at 0.64 V can be seen in the Bode plot. Since phase angle is not 45˚, it also does not follow an ideal Randles circuit.

Chapter 8

Summary and conclusion

Summary

S.1 Performance comparison for different media on T-shaped cell with optimum SPC concentartion and 0.5 M KMnO$_4$ as an oxidant concentration
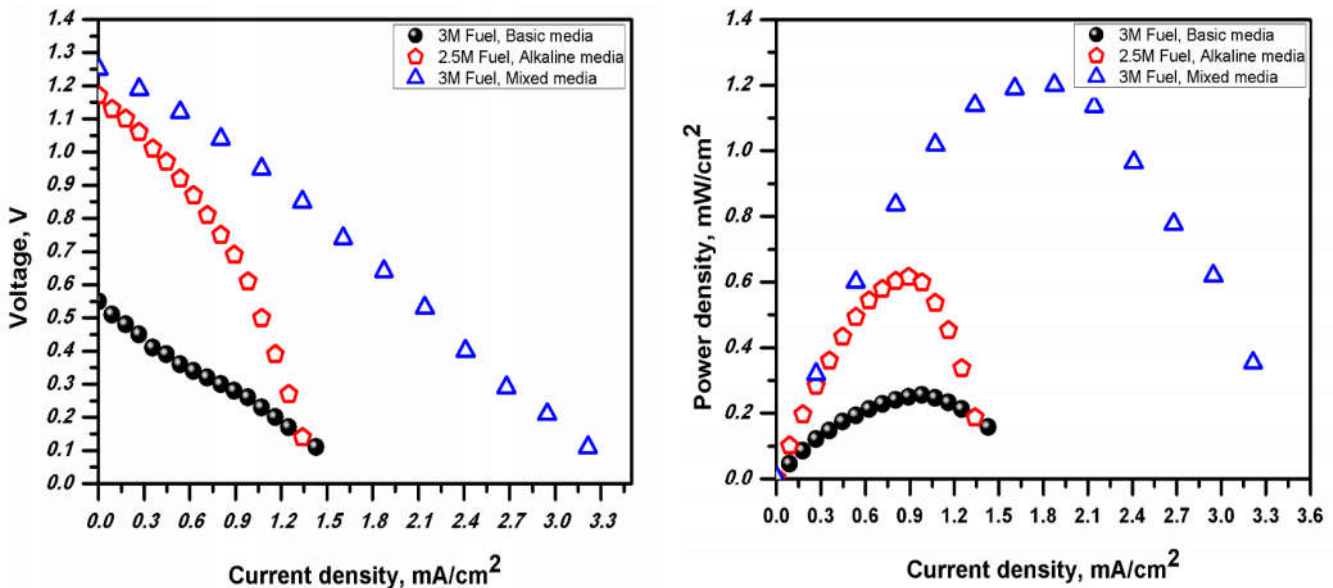
Fig S.1 Comparison of different media and the maximum performances for each media.

The above graph was plotted with an optimum 3 M SPC concentration of fuel, where the performances are maximum in the respective media.

➢ The mixed media produced current density and power density more than pure acidic or pure alkaline media. This is due to a higher theoretical OCV as well as the better ability to operate the cathode and anode at different pH.

Media Used	Current density	Power density
Acidic media	1.34 mA/cm^2	0.616 mW/cm^2
Alkaline media	1.42 mA/cm^2	0.255 mW/cm^2
Mixed media	3.21 mA/cm^2	1.2 mW/cm^2

The T-shaped mixed media outperforms the acidic as well as alkaline media. The experimental OCV (1.22 V at 3 M SPC concentration) is slightly lower than the theoretical OCV of 1.57 V.

S.2 OCV vs concentration of SPC the fuel at constant oxidant concentration (0.5 M KMnO₄) for T-shaped mixed media cells

Fuel Concentration	0.5 M	1 M	2 M	3 M
OCV	1.07 V	1.11 V	1.15 V	1.2 V

With increase in fuel concentration OCV increases due to an increase in fuel availability to the cell and due to active species concentration increase, OCV increases.

S.3 Optimization of gel electrolyte

➢ The T-shaped mixed media produced more current (*max. I = 3.08 mA*) with a 2 M-acidic gel electrolyte compared to without gel (*max. I = 0.02 mA*), due to poor ion transport in the latter.

➢ The T-shaped mixed media cell produced more current with an acidic gel membrane (*max. I = 3.08 mA*) than with an alkaline gel electrolyte (*max. I = 1.56 mA*). So the acidic gel electrolyte was preferred to perform other experiments.

➢ The 2 M-acidic gel electrolyte which gives maximum power density (1.2 mW/cm^2) and current density (3.21 mA/cm^2), which was more than at any other acidic gel electrolyte concentrations.

➢ So, the acidic gel electrolyte with a 2 M concentration is an optimized for other concentration.

➢ The conductivity of the 2 M-acidic gel electrolyte varies from, 0.06 to 0.21 (x 10^{-3} S/cm), and does remains almost same over the 10 ˚C to 90 ˚C temperature range.

S.4 T-shaped mixed media fuel cell with or without catalysts

The performance of the T-shaped mixed media cell increases with Au-NPs or Au/NiO composite (catalyst) due to increased surface area and electrical conductivity. The power density performance for the 3 M SPC fuel concentration with Au NPs as catalyst is 1.79 times more than the performance of the cell without catalyst, due to an increased surface area of gold nanoparticles. The Au/NiO composite is a better catalyst for the cell, and it gives 2.21 times more power performance than the cell without the catalyst. This is due

to porosity of the composite and dispersed NPs of gold, and these features of the composite provide more surface area as well as good electrical conductivity. Therefore the Au/NiO composite also gives much better performance than Au NPs alone.
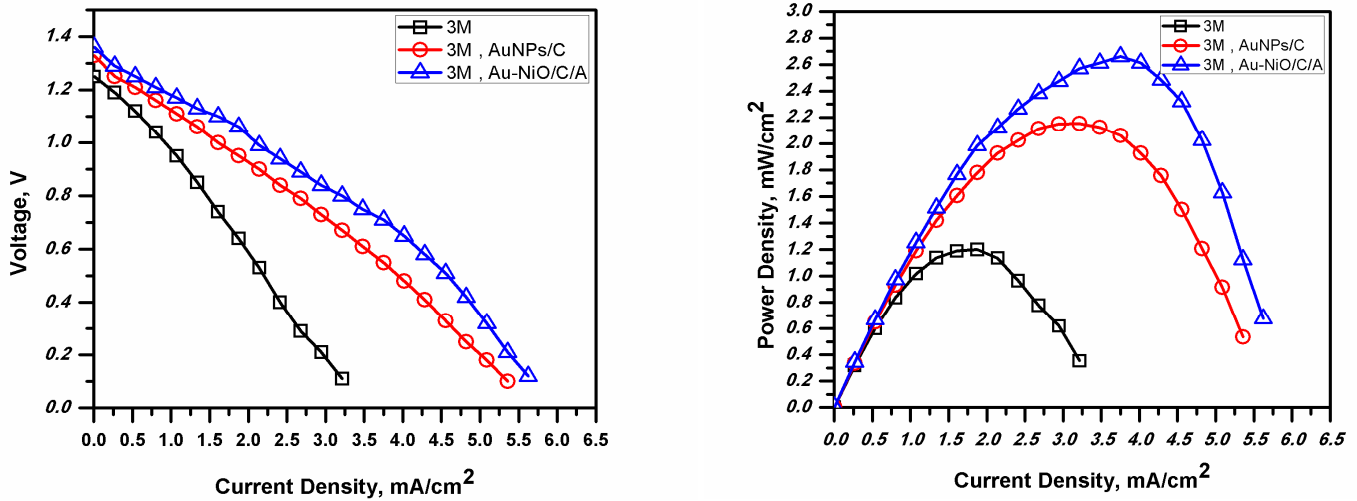
Fig S.4 Performance with and without catalyst for the T-shaped mixed media fuel cells.

Performances of the T-shaped mixed media cells with or without catalyst.

Catalyst	Current density	Power density
Without catalyst	3.2 mA/cm^2	1.2 mW/cm^2
Au-NPs	5.3 mA/cm^2	2.1 mW/cm^2
Au/NiO composite	5.6 mA/cm^2	2.6 mW/cm^2

Performance of the T-shaped mixed media cells increased with catalysts.

Cells	Increased current density	Increased power density
With Au-NPs	66.67 %	79.16 %
With Au/NiO composite	75.01 %	121.66 %

The best performance of the T-shaped mixed media paper based fuel cell is observed with the Au/NiO catalyst.

S.5 Impedance of cell with different concentrations of the SPC fuels in the T-shaped mixed media paper based fuel cells

The cell resistances decrease with increase in the concentration of the SPC fuel with same oxidant conditions.

Fig S.5 Nyquist plots for comparison of different SPC fuel concentrations with same oxidant conditions.

From fig S.5, it can be concluded that for the T-shaped mixed media paper based fuel cells, with increase in concentration of fuel from 0.5 M to 3 M, the polarization resistance of the anode decreases due to increase in fuel availability. Similarly the total resistances of the cell also decreases.
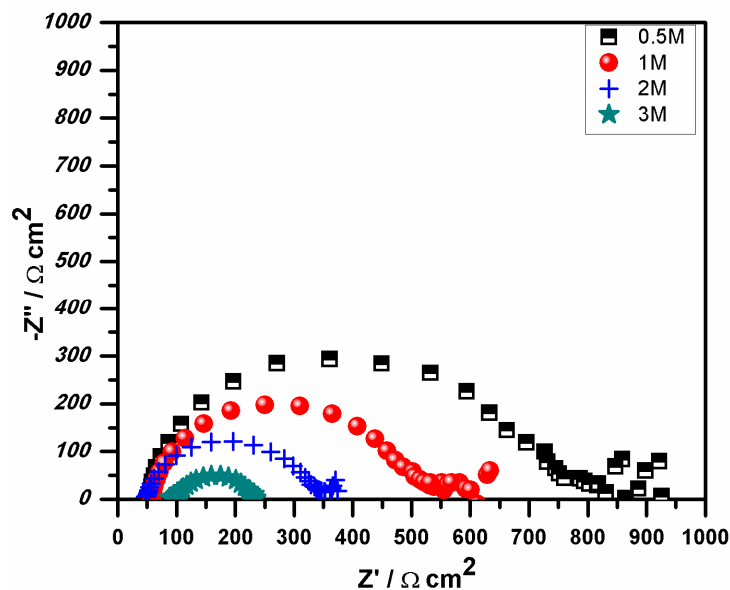
<u>Conclusion</u>

In this project, we have fabricated self-pumping T-shaped paper based fuel cells by using sodium percarbonate as a fuel and potassium permanganate as an oxidant with combination different kinds of gels and electrolyte media. This cell is light weight and consumes very less fuel. It is portable and easily accessible. Whatman filter paper was used due to its' porosity and it serves as a porous support for the fluids. The capillary action of the fluid on the porous paper allows the parallel streams of anolyte and catholyte. The mixed media and acidic gel-electrolyte combination based cell outperforms the pristine acidic and basic media based cell. The former gives a high OCV (1.22 V at 3 M SPC fuel). The T-shaped mixed media paper based fuel cell produces a maximum current density of 3.21 mA/cm^2 and a maximum power density of 1.2 mW/cm^2 without any catalyst. Au NPs used as catalyst shows sudden increase in the current and power densities due to their good catalytic properties. 66.67 % and 79.16 % of increase in current density and power density respectively were observed when Au-NPs were used as catalysts. We also tried Au/NiO composite as a catalyst on the T-shaped mixed media paper based fuel cell which increases the performance of the cell due to its' porous morphology. The Au/NiO composite as catalyst increases current and power densities by 75.01 % and 121.66 % respectively. From EIS studies, it was concluded that with the increase in SPC fuel concentration at anode and constant oxidant condition at cathode, the anodic polarization resistances decreases. The total resistance of the cell decreases with increase in fuel concentration.

The T-shaped mixed media paper based fuel cell produces sufficient voltage, current density as well as power density and thus can be used to operate any micro-nano-system (devices) like diagnostic strips, remotes for one time use, laser locater as indicator source for sensitive area, digital timer as well as to illuminate LED bulb for short duration applications etc. Further, stacks of these cells can be made which would be able to fulfill the power equivalent of higher voltage electrical devices which could be used for more than half an hour and can be disposed easily. The goal of this project was not only inclined towards power generation but also to deliver a cell which is environmental friendly as well as conveniently disposable with less harmful or harmless byproducts.

References

[1] L. Carrette, K.A. Friedrich and U.Stimming, Fuel Cells-Fundamentals and applications. Wiley review, Fuel Cells, **1**, 5-39 (2001).

[2] M. Stanley Whittingham, Robert F. Savinell, Thomas Zawodzinski, Introduction: Batteries and Fuel Cells. Chem. Rev.*,* **104**, 4243–4244 (2004).

[3] Wipke, Keith, Sam Sprik, Jennifer Kurtz and Todd Ramsden, Hydrogen and Fuel Cell Vehicles Worldwide. TÜV SÜD Industry Service GmbH (2011). Controlled Hydrogen Fleet and Infrastructure Demonstration and Validation Project, National Renewable Energy Laboratory (2011)

[4] J.M. Andujar, F. Segura, Fuel cells: History and updating. A walk along two centuries. Renewable and Sustainable Energy Reviews, **13**, 2309–2322 (2009).

[5] J.P. Esquivel, F. J. del Campo, J.L. Gomez de la Fuente, S. Rojas and N. Sabate, Paper-Based Microfluidic Fuel Cells. RCS, 1251-1253 (2013).

[6] Mark C. Williams, Fuel Cell Handbook, Seventh Edition, EG&G Technical Services, Inc. (2004)

[7] Chris Rayment and Scott Sherwin, Introduction to Fuel Cell Technology (2003).

[8] K.R. Cooper, M. Smith, Electrical test methods for on-line fuel cell Ohmic resistance measurement. Journal of Power Sources, **160**, 1088–1095 (2006).

[9] Electrochemical impedance spectroscopy, http://www.gamry.com and http://nptel.ac.in/courses/103102015/fuel%20cell%20characterization/in%20situ%20characterization.html

[10] Yugang Sun and Younan Xia, Gold and silver nanoparticles: A class of chromophores with colors tunable in the range from 400 to 750 nm. RCS, Analyst, **128**, 686–691 (2003).

[11] Roberto Cesareo, X-Ray Fluorescence Spectrometry. Wiley, **39**, 595-631 (2012).

[12] Ravi Kumar Arun, Saurav Halder, Nripen Chanda and Suman Chakraborty, A paper based self-pumping and self-breathing fuel cell using pencil stroked graphite electrodes. Lab Chip, **14**, 1661–1664 (2014).

[13] J. P. Esquivel, F. J. Del Campo, J. L. Gomez de la Fuente, S. Rojas and N. Sabate, Microfluidic fuel cells on paper: meeting the power needs of next generation lateral flow devices. Energy Environ. Sci., **7**, 1744-1749 (2014).

[14] Patent CN104671387A, Method for removing BTEX out of underwater through novel sodium percarbonate oxidizing agent (2015).

[15] Qunwei Tang, Guoqing Qian and Kevin Huang, H_3PO_4-imbibed three-dimensional polyacrylamide/polyacrylamide hydrogel as a high-temperature proton exchange membrane with excellent acid retention, RSC Adv., **2**, 10238–10244 (2012).

[16] Myron A. Smith, A Consideration of Graphite Electrodes. IEEE, Transactions On Industry Applications, **18**, 431-434 (1982).

[17] Erik Kjeang, Jonathan McKechnie, David Sinton and Ned Djilali, Planar and three-dimensional microfluidic fuel cell architectures based on graphite rod electrodes. Journal of Power Sources, **168**, 379–390 (2007).

[18] Alaxander McKillop and William R Sanderson, Sodium borate and sodium percarbonate: cheap, safe and versatile oxidizing agent for organic synthesis. Tetrahedron, **51**, 6145-6166 (1995).

[19] Steven G. Bratsch, Standard electrode potentials and temperature coefficients in water. J. Phys. Chem. Ref. Data, **18**, 1-21 (1989).

[20] M. Gowdhamamoorthi, A. Arun, S. Kiruthika and B. Muthukumaran, Enhanced Performance of Membraneless Sodium Percarbonate Fuel Cells. Journal of Materials, 1-7 (2013).

[21] K. Ponmani, S. Durga, M. Gowdhamamoorthi, S. Kiruthika and B. Muthukumaran, Influence of fuel and media on membraneless sodium percarbonate fuel cell. Springer, **20**, 1579-1589 (2014).

[22] Haibing Xia, Shuo Bai, Jurgen Hartmann and Dayang Wang, Synthesis of Monodisperse Quasi-Spherical Gold Nanoparticles in Water via Silver (I)-Assisted Citrate Reduction. Langmuir, **26**, 3585–3589 (2010).

[23] F. Pei, Y. Wang, X. Wang, P. Y. He, L. Liu, Y. Xu, and H. Wang, Preparation and Performance of Highly Efficient Au Nanoparticles Electrocatalyst for the Direct Borohydride Fuel Cell. Wiley, Fuel Cells, **11**, 595–602 (2011).

[24] Lu Pan, Liying Shen, Li Li, Qiyong Zhu, Synthesis of Au/NiO hollow micro-spheres and their adsorption and electrocatalytic properties for p-nitrophenol. J Mater Sci: Mater Electron, **27**, 3065–3070 (2016).

[25] C.M. Lampert, T.R. Omstead and P.C. Yu, Chemical and optical properties of electrochromic nickel oxide film. Solar energy materials, **14**, 161-174 (1986).

[26] Xiuling Yan, Fanhui Meng, Yun Xie, Jianguo Liu and Yi Ding, Direct N_2H_4/H_2O_2 Fuel Cells Powered by Nanoporous Gold Leaves. Science reports, **2**, 1-7 (2012).

[27] Sweta Lal, Vinod M. Janardhanan, Melepurath Deepa, Anand Sagar and Kirti Chandra Sahu, Low Cost Environmentally Benign Porous Paper Based Fuel Cells for Micro-Nano Systems. Journal of The Electrochemical Society, **162**, F1402-F1407 (2015).

[28] Omar Z. Sharaf and Mehmet F. Orhan, An overview of fuel cell technology: Fundamentals and applications. Renewable and Sustainable Energy Reviews, **32**, 810–853 (2014).